Western&Graduate&PostdoctoralStudies

Electronic Thesis and Dissertation Repository

8-20-2020 11:00 AM

The Study of Bubble Growth Hydrodynamics in the Supersaturated Liquids

Raj Kumar Nayak Maloth, *The University of Western Ontario*

Supervisor: Khayat, Roger E, *The University of Western Ontario*
Joint Supervisor: DeGroot, Christopher T, *The University of Western Ontario*
A thesis submitted in partial fulfillment of the requirements for the Master of Engineering Science degree in Mechanical and Materials Engineering
© Raj Kumar Nayak Maloth 2020

Follow this and additional works at: https://ir.lib.uwo.ca/etd

Part of the Other Mechanical Engineering Commons

Abstract

Bubble formation and dissolution have a wide range of industrial applications, from the production of beverages to foam manufacturing processes. The rate at which the bubble expands, or contracts has a significant effect on these processes. In the current work, the hydrodynamics of an isolated bubble expanding due to mass transfer in a pool of supersaturated gas-liquid solution is investigated. The complete scalar transportation equation (advection-diffusion) is solved numerically and it has been observed that the present model predicted an accurate bubble growth when compared with existing approximated models and experiments. The effect of gas-liquid solution parameters such as inertia, viscosity, surface tension, diffusion coefficient, system pressure, and solubility of the gas has been investigated. It is found that the surface tension and inertia have a very minimal effect during the bubble expansion. However, it is observed that the viscosity, system pressure, diffusion, and solubility have a considerable effect on bubble growth.

Keywords

Summary for Lay Audience

The current thesis investigates the growth of a single bubble in a mixture of supersaturated gas-liquid solution. A solution is said to be supersaturated when the amount of gas dissolved in the solution is more than it can hold. The growth and control of bubbles play a key role in industrial applications such as bubble column reactors where gas is dissolved in the liquid in terms of bubbles, daily consumable beverages where CO_2 is suspended as bubbles, manufacturing processes where thermoplastic foams are produced using blowing agents, and in marine commutators where the collapse of high-pressure bubbles causing damage to propeller blades of the ships. In the literature, the governing equation which describes the concentration of gas in the liquid is solved with many underlying assumptions and simplifications. In the present study, this complete equation is solved numerically and compared with the existing theory and experiments. The present numerical approach is validated by reproducing the results in the literature. It has been depicted that the present theory matched closely with the experiments than the existing theories.

Acknowledgments

Foremost, I am grateful to my mother, father, and my brothers for their love and support throughout my life.

Firstly, I would like to express my sincere gratitude to my supervisors Dr. Roger Khayat and Dr. C.T. DeGroot for their continuous support in the completion of this thesis. I am indebted to Dr. Khayat for his constant encouragement, mental support, and for pushing me to widen my knowledge in the field of fluid mechanics and related area. I would like to thank Dr. DeGroot for his important inputs and guidance during my difficult situations in the research.

Secondly, I would like to thank my uncle Mr. B. Harisingh for his strong support and inspiration. I take this opportunity to thank my friends and co-researchers: Dwaipayan Sarkar, Glen Dsouza, Shoyon Panday, and Yunpeng Wang for their thoughtful feedback and constant support during my master's journey. More importantly, I thank Gayathri Aryasomayajula for being with me in the ups and downs of my masters' endeavour.

Finally, I thank again Dr. Roger and Dr. DeGroot for giving me this wonderful opportunity to work under their esteemed supervision.

Table of Contents

List of Tables

List of Figures

Nomenclature

$\bar{c}$	Mass fraction of gas in the liquid
$\bar{c}_R$	Mass fraction of gas at the interface
c_0	Saturation /initial mass fraction of gas in the liquid
c_s	Supersaturated mass fraction of gas in the liquid
Ca	Capillary number
D	Diffusion coefficient, m^2 / s
I	Non-dimensional Solubility number
i	Node index
k_h	Henry's constant, m^2 / N
M	Molecular weight of the gas, kg / mol
N	Total Number of nodes
$\vec{n}$	Unit normal vector
$p_g(t)$	Pressure of the gas in the bubble
p_0	Saturation pressure of the gas in the liquid
$p_R(t)$	Pressure of gas at the bubble interface
p_a	Pressure of a system or ambient pressure
p_h	Undersaturated pressure of a gas
$\bar{p}_{g0}$	Dimensional initial pressure of the gas, N/ m^2
p_s	Supersaturated pressure of a gas

Pe	Peclet number
$\bar{R}(\bar{t})$	Dimensional radius of the bubble, m
$\bar{R}_0$	Dimensional initial radius of the bubble, m
$\dot{\bar{R}}$	Dimensional interface velocity of the bubble, m/s
R_g	Universal gas constant, $J/\text{mol}-K$
$\dot{R}$	Interface velocity of the bubble
Re	Reynolds number
$\bar{S}$	Shell thickness, m
$\bar{S}_0$	Dimensional initial shell thickness, m
T_0	Saturation temperature of a gas
T_s	Supersaturation temperature of a gas
T_h	Undersaturated temperature of a gas
T	Temperature of a gas
$\bar{t}$	Dimensional time, s
t	Time
$\bar{t}_{ref}$	Reference time, s
$\bar{u}_\theta$	Dimensional angular velocity component, m/s
$\bar{u}_\phi$	Dimensional azimuthal velocity component, m/s
$\bar{u}_r$	Dimensional radial velocity component, m/s
$\bar{V}_c$	Volume of the shell, m^3

$\overline{V}$	Characteristic velocity of the liquid, m/s
$\overline{x}(r,t)$	Mapped Domain coordinate, m
y_N	System of ordinary differential equations
Z	Non-dimensional number
ρ_g	Density of gas, kg/m^3
ρ_L	Density of liquid, kg/m^3
$\overline{\delta}$	Boundary layer thickness, m
σ	Surface tension of the liquid, N/m
$\overline{\tau}_{rr}$	Dimensional radial normal stress, N/m^2
$\overline{\tau}_{\theta\theta}$	Dimensional angular normal stress, N/m^2
λ	Stress relaxation factor
μ_L	Viscosity of the liquid, $pa.s$
θ	Angular direction
ϕ	Azimuthal direction

Chapter 1

1 Introduction

1.1 Introduction to topic

A gas bubble is formed when an atomically or molecularly dissolved gas becomes supersaturated in a liquid solvent as a result of the reduction in imposed gas pressure, or change in liquid temperature and or change in solute or solvent character (Rosner and Epstein, 1972). The study of the gas bubble is of major interest due to its appearance in many real-world problems, where the formation of the bubbles in some applications is desired and some of them not. For an instant, the dissolved oxygen in the bioreactors in the form of bubbles is the desired process (see the red circle marked in figure 1-1 a), whereas the formation of gas bubbles near the propeller blades of the ships is an undesired effect (due to which the blades get corroded rapidly (see the red area marked in figure 1-1 b)).

(b)

(a)
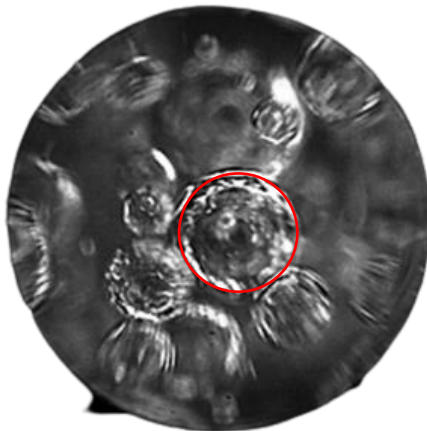
Figure 1-1: Effects of the bubble in a) bioreactors (Hernandez-Alvarado et al., 2017) and b) ship propeller blades (PES Solutions, 2014)

In the current chapter, we begin by explaining how bubble formation and dissolutions are important in various industrial applications. Thereafter, a clear problem description will be made followed by explaining the important terms of supersaturation and undersaturation. Later in the chapter, an intensive literature survey will be carried out discussing the various bubble growth models and highlighting their limitations and assumptions. Finally, the chapter will end by briefing the research gaps and thesis outline.

1.2 Practical Applications

One of the important applications of bubble hydrodynamic theory is in chemical process industries, where the foamed plastics (see figure 1-2) production is one of the major aspects (Elshereef et al., 2010). When a gas-generating substance like a blowing agent is mixed with the high-pressure molten polymer, the resulting product turns out to be thermoplastic (Arefmanesh et al., 1992). In this process, gas bubbles emerge and have a considerable effect on product quality. Therefore, it is necessary to understand the behavior of bubbles under different process parameter conditions.
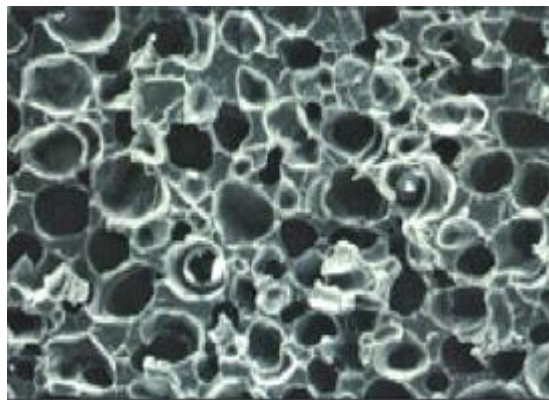
Figure 1-2: Plastic Foams (Elshereef et al., 2010)

High-density foamed thermoplastics, otherwise called as cellular plastics, are used in household furniture, transportation, and building products, and on the other hand, low-

density thermoplastics are frequently used in rigid packing (Lee et al., 1996). Bubble hydrodynamics plays a key role in the dry-photography of documents, where the process requires the light-scattering bubbles in a plastic medium (Barlow and Langlois, 1962). Bubble hydrodynamics plays a vital role in the design and scale-up of a bubble column reactors (Wild, 2003).

The formation and growth of bubbles due to de-gassing or reduction of pressure in a supersaturated gas-liquid solution is observed in a broader spectrum of industrial and natural processes. For example, a very well-known process in which de-gassing is observed are carbonated beverages, such as beers, gushing in soda, and champagne (Bisperink and Prins, 1994; Jones et al., 1999; Barker et al., 2002; Liger-Belair, 2005; Lee et al., 2011; Enríquez et al., 2013, 2014). Another example, from the biological perspective, includes bubble growth in blood and tissues due to decompression sickness (Chappell and Payne, 2006). From the environmental perspective, bubble growth due to de-gassing in magmas during the volcanic eruption (Sparks, 1978) and while boiling the cryogenic solutions has a major impact (Kuni and Zhuvikina, 2002; Zhuvikina and Kuni, 2002; Kuni et al., 2003). The study of bubble dynamics is vital in production industries, where molten polymers, metals, and glasses are of major interest (Amon and Denson, 1984) and a bubble prediction theory is important in the exsolution of gases during oil extraction (Pooladi-Darvish and Firoozabadi, 1999).

The importance of bubble growth in the industrial processes turned the researcher's attention to study its behavior and control. But the accurate prediction of this process became very complicated because of its complex physics, which requires coupling hydrodynamics to the diffusion process. The bubble growth process exhibits different

regimes where different flow parameters take control over the growth; for instance, after immediate nucleation, surface tension plays a significant role and at initial growth, inertia takes the control and at later stages, the bubble evolves due to diffusion process.

The early analytical models of the bubble growth process in supersaturated solutions were developed with many assumptions. Such as, neglecting the inertia of the liquid and neglecting the convective effect produced due to motion of the bubble boundary (Epstein and Plesset (1950)) and some studies have not prioritized viscosity of the liquid and pressure jump across the bubble interface (Scriven (1959)).

1.3 Problem Description

When the pressure of the dissolved gas in a liquid solution is decreased to a certain level, bubbles tend to nucleate on the surface of cracks, pores in a pool of gas-liquid solution. The current study is not focused on the bubble nucleation; rather, it focusses on a single gas bubble growth that is previously nucleated in a pool of liquid-gas supersaturated solution (see figure 1-3).
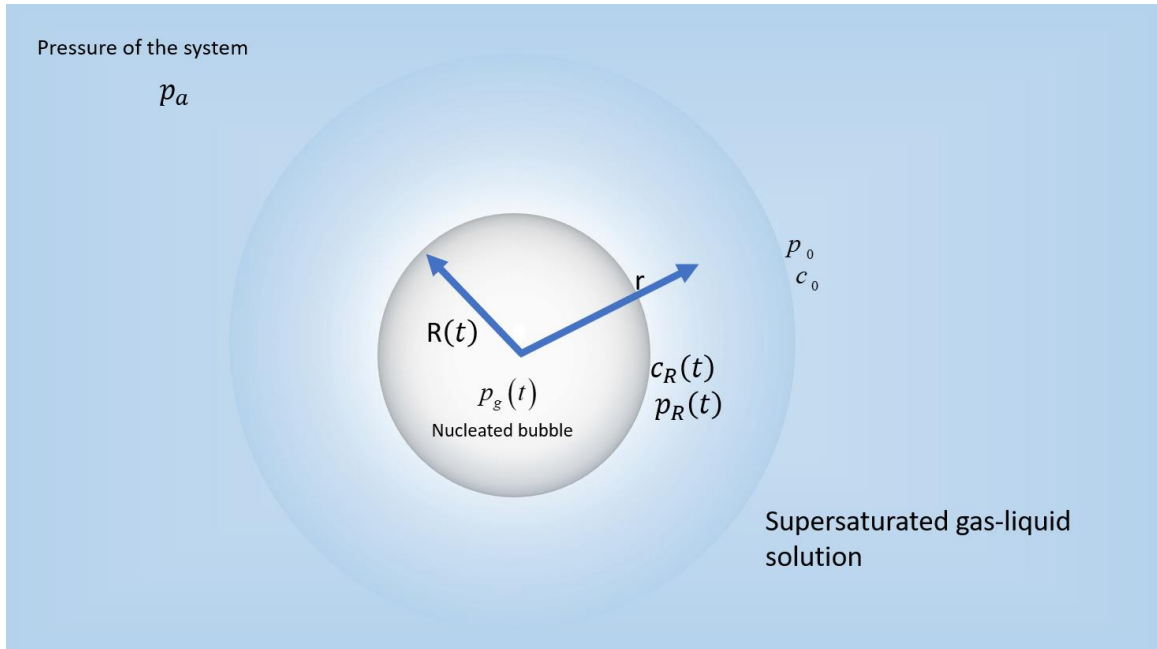
Figure 1-3: Schematic representation of the problem

Here c_0 is the initial or saturation concentration far from the bubble and p_0 is its corresponding partial pressure. On the other side $p_g(t)$ is the pressure of the gas inside the bubble and $p_R(t)$ is the pressure at the interface of the bubble and p_a is the external pressure on the liquid or pressure of the system (for example mold pressure in the mold injection foaming process).

The present study emphasis developing a numerical model that comprises all interfacial, inertial, and viscous effects and providing a clear insight into the behavior of gas concentration in the liquid. Moreover, this study also focuses on including the nonlinear convective terms in the diffusion equation which have been neglected by many researchers.

To understand the bubble growth process, it is important to get an idea of the supersaturation and undersaturation process in a gas-liquid solution. In the subsequent section, this will be discussed.

1.4 Supersaturation and Undersaturation

When gas is dissolved in the liquid, the liquid reaches its saturation point; i.e. it cannot hold more gas after that point. Let the amount of dissolved gas, its partial pressure, and temperature at the saturation point be c_0, p_0 and T_0. Now to increase the gas holding capacity of the liquid, one can reduce the pressure from the saturation pressure p_0 to new pressure p_s or increase the temperature from the saturation temperature to a new temperature T_s. At these new conditions where pressure is p_s or the temperature is T_s, the liquid holds more gas (c_s) than at its saturation point. At this point, gas always tries to escape from the solution to reach its saturation or equilibrium position c_0. This new condition where liquid holds more gas than its equilibrium or saturation condition is termed as supersaturation or over-saturation condition.

Conversely, one can increase the pressure to p_h or decrease the temperature T_h. At these conditions, the liquid tries to absorb more gas from its surroundings; this is termed as undersaturation.

The amount of gas that liquid can absorb or release from its surroundings can be determined by the dimensionless saturation ratio ζ (Moreno Soto et al., 2019).

$$\zeta = \frac{c_0 - c_s}{c_s} \tag{1.1}$$

In equation (1.1) $\zeta > 0$ represents the level of supersaturation and $\zeta < 0$ determines the level of undersaturation and the saturation or equilibrium condition is represented as $\zeta = 0$. In the present study, we focus on the supersaturation level i.e. $\zeta > 1$.

1.5 Literature Survey

In the current section, theoretical and numerical models that were developed in the literature for a bounded and unbounded single spherical gas bubble in a supersaturated or undersaturated liquid will be detailed. Also, the assumptions, solution producer, numerical complications, and solution accuracy challenges in the literature are addressed.

In many industrial applications, bubble growth is driven by mass transfer (Payvar, 1987; Wang and Bankoff, 1991; Bisperink and Prins, 1994; Hey et al., 1994; Jones et al., 1999; Barker et al., 2002; Lin et al., 2002; Divinis et al., 2004). Epstein & Plesset, (1950) derived an approximate analytical solution to an unbounded single bubble growth/dissolution in a gas-liquid solution due to mass transfer for supersaturated and undersaturated conditions. Their approximate solution emerges by neglecting a transport term in the advection-diffusion equation; this transport term results from the boundary motion of the bubble. However, the approximate solution procedure which they obtained is a very complicated process and for a fast-growing bubble these solution underpredicts the growth.

Epstein and Plesset (1950) solved the one-dimensional advection-diffusion equation without an advection term, which is analogous to the one-dimensional transient heat conduction equation and is given by

$$\frac{\partial \overline{c}}{\partial \overline{t}} = D\left(\frac{2}{\overline{r}} \frac{\partial \overline{c}}{\partial \overline{r}} + \frac{\partial^2 \overline{c}}{\partial \overline{r}^2} \right). \tag{1.2}$$

Note that the variables or parameters with the bar represent the dimensional number. Here $\overline{c}\left(\overline{r},\overline{t}\right)$ is the gas concentration in the liquid, $\overline{r}$ is the radial position and D is the

diffusion coefficient of gas. Epstein and Plesset (1950) used the Carslaw (1945) solution

of 1d heat conduction problem (equation (1.2)) which is written as

$$\bar{c}\left(\bar{\xi},\bar{t}\right) = \frac{\bar{c}_0 - \bar{c}_R}{\sqrt{2\pi D\bar{t}}} \int\limits_0^\infty \left(\bar{R} + \xi'\right) \left\{ \exp\left[-\frac{\left(\bar{\xi} - \bar{\xi'}\right)^2}{4D\bar{t}} \right] - \exp\left[-\frac{\left(\bar{\xi} + \bar{\xi'}\right)^2}{4D\bar{t}} \right] \right\} d\bar{\xi'},$$

(1.3)

here $\bar{\xi} = \bar{r} - \bar{R}\left(\bar{t}\right)$ is the transformed coordinate used in the solution procedure. Here

$\bar{R}\left(\bar{t}\right)$ is the bubble radius, $\bar{c}_0$, $\bar{c}_R$ are the saturation concentration and interface

concentrations respectively. Epstein and Plesset used equation (1.3) to determine the

concentration at the interface of the bubble as

$$\left(\frac{\partial \bar{c}}{\partial \bar{r}} \right)_{\bar{R}} = \left(\bar{c}_0 - \bar{c}_R\right)\left(\frac{1}{\bar{R}} + \frac{1}{\sqrt{\pi D\bar{t}}} \right).$$

(1.4)

Equation (1.4) is the key finding of Epstein and Plesset, which describes the bubble growth

as a function of the boundary layer around the bubble which has a thickness equal to

$\sqrt{\pi D\bar{t}}$. The final form of the Epstein and Plesset equation is written as

$$\bar{R}(t) \approx \left(\sqrt{\left(\frac{\bar{c}_0 - \bar{c}_R}{2\pi\rho_g} \right)} + \sqrt{1 + \left(\frac{\bar{c}_0 - \bar{c}_R}{2\pi\rho_g} \right)} \right) \sqrt{\frac{2D\left(\bar{c}_0 - \bar{c}_R\right)}{\rho_g}\bar{t}} .$$

(1.5)

Equation (1.5) describes a pure diffusive bubble growth in a supersaturated solution whose

density of the gas is ρ_g , with initial equilibrium concentration being $\bar{c}_0$ and the

supersaturated concentration being $\bar{c}_R$ (at the interface the magnitude of the concentration

is equal to supersaturation concentration). Epstein's formulation suggests that the bubble grows as the square root of time i.e $\bar{R} \propto \sqrt{t}$.

The study of bubble dynamics is not only important in the pure mass transfer phenomenon but also plays a vital role in nucleate boiling processes (Plesset and Zwick, (1954); Birkhoff et al., (1958); Scriven, (1959); W.Zijl, D.Moalem, (1977); Prosperetti and Plesset, (1978); Verhaart et al., (1980)). Scriven (1959) derived an approximate solution for the bubble growth in the boiling process; they included the convective term in the diffusion equation which was neglected by Epstein and Plesset (1950). However, Scriven made the following assumptions:

1. Neglected the viscosity effect of the liquid on the bubble growth stating that it only plays important role at initial stages,

2. Omitted the inertial and interfacial effect of liquid on bubble growth.

Scriven's (1959) bubble dynamics formulations are quite complicated and have many underlying assumptions. However, the present thesis does not deal with the boiling process; this information is provided only to understand the broader perspective of bubble dynamics.

Barlow and Langlois (1962) investigated a bubble expanding in a Newtonian liquid due to the diffusion of nitrogen gas from vinylidene chloride-acrylonitrile copolymer. They introduced a very complicated Integro-differential equation based on a thin shell assumption that describes the combined hydrodynamic and diffusion growth of the bubble. They had analyzed the bubble growth in two extreme conditions, one of them being the very slow diffusion of gas in the bubble where they neglected inertia of liquid and

developed an asymptotic solution for bubble growth and the other being the rapid diffusion process, where the pressure in the bubble remains almost constant and is controlled by pure hydrodynamics.

Barlow and Langlois (1962) concluded that their approximate solutions at the initial and final stages will be applicable for a bubble that grows at a very short period (less than 2 seconds). They also admitted that solving their system of equations is computationally very expensive and needs a lot of arithmetic operations to predict small bubble growth. However, Barlow and Langlois (1962) were the first to combine the hydrodynamics and diffusion effects. Their model is complicated and time expensive to use for the larger bubble growth rates.

Rosner and Epstein (1972) laid a strong fundamental pavement in the field of diffusive controlled bubble growth. They developed a hydrodynamic formulation based on the moment integral method. Their investigation accounts for the ratio of the density of the gas to the density of the liquid $\left(\dfrac{\rho_g}{\rho_L} \right)$ that appears in the kinematic condition at the interface and the convection part in the diffusion equation which is induced by the motion of the bubble interface. However, they assumed the pressure inside the gas bubble to be constant.

Rosner and Epstein (1972) assumed a parabolic concentration profile in a thin boundary layer to generate an approximate solution of the diffusion equation. This work has been adopted by many researchers starting from Patel (1980), Han and Yoo (1981) to Elshereef et al., (2010). Rosner has investigated the effects of interface kinetics, solute diffusion, and

surface tension on the bubble growth and concluded that bubble growth depart from classical behavior $\bar{R} \propto \sqrt{t}$.

Bubble formation in the manufacturing processes of foaming material is one of the foremost interests among the researchers. When a molten polymer is injected with high pressure inside the mold, the bubble nucleates and starts expanding. Patel, (1980) developed a bubble growth model in a supersaturated Newtonian liquid. The main idea behind Patel's bubble growth model is to make the formulations simple compared to Barlow et al. (1962) and Rosner et al. (1971). He focused on a single gas bubble that is nucleated in a pool of liquid with the following assumptions:

1. The liquid is Newtonian with constant viscosity,

2. The process is isothermal and always exits a thermodynamic equilibrium at the gas-liquid interface which obeys Henry's law,

3. The liquid is stagnant and of infinite extent,

4. A large pool of liquid is available, and gas is abundant,

5. A thin boundary layer $\bar{\delta}$ is formed around the bubble in which the variation of gas concentration is observed,

6. The ratio of the boundary layer $\bar{\delta}$ to the instant bubble radius $\bar{R}(t)$ is very small i.e $\dfrac{\bar{\delta}}{\bar{R}} << 1$,

7. The gas concentration after the immediate vicinity to the boundary layer is equal to the saturated concentration.

Patel's boundary layer thickness $\bar{\delta}$ emerges by solving the diffusion equation analytically with the help of Rosner and Epstein's (1971) parabolic concentration profile assumption. Note that the explicit derivation of boundary layer thickness and the approximate solution to the advection-diffusion equation is detailed in chapter two.

The molten polymer in the foaming process exhibits viscoelastic behavior (Arefmanesh and Advani, 1991; Khayat and Garcia-Rejon, 1992; Venerus and Yala, 1997; Venerus et al., 1998; Allen and Roy, 2000; Feng and Bertelo, 2004; Brujan and Williams, 2005; Jiménez-Fernández and Crespo, 2005; Xu et al., 2005). The formation of bubbles is often observed in the foaming manufacturing process. As discussed earlier, Barlow et al., (1962) and Patel (1980) developed models for pure Newtonian fluid cases, hence neglected the effect of the elastic nature of the polymer. To fill this gap, Han and Yoo (1981) introduced a model that includes the effect of elasticity of the fluid (polymer). They also experimentally studied the bubble growth when a gas-charged molten polymer is injected into the mold cavity in the mold injection process.

Han and Yoo used sodium bicarbonate as a blowing agent, which generates carbon dioxide (CO_2) gas in the molten polymer. They experimented at isothermal conditions keeping the fluid properties constant while varying injection rates. They noticed that bubble formation is observed at a particular injection rate. To incorporate the effect of elasticity they used a viscoelastic model represented by DeWitt. The Stress relaxation, diffusion, and interfacial effects were incorporated in their theoretical model; therefore, the hydrodynamic equation of Han and Yoo is given as

$$\rho_L \left(\ddot{R}\overline{R} + \frac{3}{2}\dot{\overline{R}}^2 \right) = \overline{p}_g - \frac{2\sigma}{\overline{R}} - \overline{p}_a + \overline{\tau}_{rr(\infty)} - \overline{\tau}_{rr(R)} + 2\int_R^\infty \frac{\overline{\tau}_{rr} - \overline{\tau}_{\theta\theta}}{r} d\overline{r} .$$ (1.6)

Here ρ_L and σ are density and surface tension of the liquid, $\overline{\tau}_{rr}$ and $\overline{\tau}_{\theta\theta}$ are normal stress in radial and angular direction and their behavior is given by the DeWitt Model which are represented as

$$\overline{\tau}_{rr} + \lambda \left(\frac{\partial \overline{\tau}_{rr}}{\partial \overline{t}} + \overline{u}\frac{\partial \overline{\tau}_{rr}}{\partial \overline{r}} \right) = 2\mu \frac{\partial \overline{u}}{\partial \overline{r}} ,$$ (1.7)

$$\overline{\tau}_{\theta\theta} + \lambda \left(\frac{\partial \overline{\tau}_{\theta\theta}}{\partial \overline{t}} + \overline{u}\frac{\partial \overline{\tau}_{\theta\theta}}{\partial \overline{r}} \right) = \frac{2\mu\overline{u}}{\overline{r}} ,$$ (1.8)

With λ being the stress relaxation term, μ being the viscosity of the liquid, and u is the radial velocity.

Han and Yoo determined $\overline{p}_g$ in the equation (1.6) with the same approach followed by Patel (1980). Note that in the absence of stress relaxation term λ, Han and Yoo's model reduces to the Newtonian hydrodynamic model.

The stress builds up in the polymer during its injection in the mold has a significant effect on bubble formation and bubble growth. This is one of the key observations presented by Han and Yoo. At low injection pressure, they observed that the elasticity of the polymer melt helps in bubble growth, whereas at high injection pressure the bubble growth is highly retarded. Therefore, the rate of bubble growth depends on the elasticity of the melt and the injection pressure.

Polymer foams material has abundant importance in the commercial industries starting from high thermal insulators like glass fibers to high rigid material in structural maintenance (Amon and Denson, 1984). These polymers can be produced with a wide range of manufacturing processes like injection molding to extrusion (Harris, 1976). In all these manufacturing processes a common phenomenon of formation and growth of bubbles is observed. Amon and Denson (1984) investigated the bubble growth theoretically in the foaming process.

To this point in our survey, researchers have investigated the bubble dynamics in a pool of liquid based on the abundant gas availability assumption. This assumption is adequate for the bubbles separated by a larger distance. On the other hand, when bubbles are formed in closed proximity, i.e. the distance between the bubbles is smaller than their radius, the infinite availability of gas assumption will no longer hold (Amon and Denson 1984). Therefore, Amon and Denson's theoretical model incorporates the effect of available gas from the surrounding bubbles. Their analysis is developed on a cell model assumption, where they have considered the foam as a summation of an equal microscopic unit of spherical cells with a constant mass in it and every cell has a spherical gas bubble that grows by diffusion of gas from the microscopic unit (see figure 1.4).
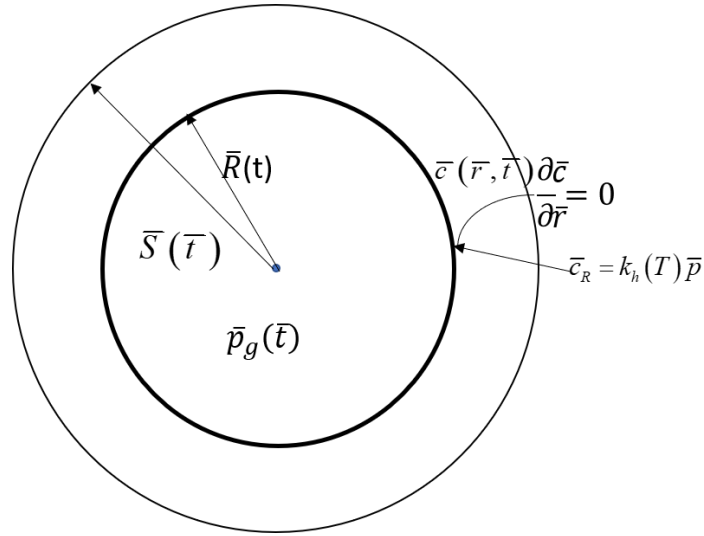
Figure 1-4: Schematic view of a unit cell (Amon and Denson 1984)

The non-inertial isothermal theoretical model of Amon and Denson (1984) in terms of volume of the shell is written as

$$\frac{d\bar{R}}{d\bar{t}} = \frac{\bar{V}_s + \bar{R}^3}{4\mu\bar{V}}\left[\left(\bar{p}_g(t) - \bar{p}_a\right)\bar{R} - 2\sigma\right] \; , \tag{1.9}$$

Here $\bar{V}_s$ is the volume of the shell. Amon and Denson captured the transient behaver of $\bar{p}_g(t)$ by solving the advection-diffusion equation (see equation (2.28)) numerically. In the current thesis work, a similar methodology of Amon and Denson is adopted for the solution $\bar{p}_g(t)$.

Following Han and Yoo, Ramesh *et al.*, (1991) investigated the bubble hydrodynamics in the thermoplastics. Their study comprises of experimentation and theoretical model development. Ramesh et al., (1991) primarily focused on studying the effect of saturation pressure, blowing agent, the temperature of a gas, and molecular weight of the gas on bubble growth. They modified an existing Newtonian hydrodynamic formulation (see

equation 1.6) of a single bubble growing in an infinite polymer solution to account for the non-Newtonian effect by considering the polymer as a power-law fluid which is written as

$$\rho_L \left(\ddot{R}\bar{R} + \frac{3}{2}\dot{\bar{R}}^2 \right) = \bar{p}_g - \frac{2\sigma}{\bar{R}} - \bar{p}_a - \frac{4K\left(2\sqrt{3}\right)^{(n-1)}}{n}\left(\frac{\dot{R}}{R}\right)^n,$$ (1.10)

In equation (1.10) K and n are the power-law parameters and have different values for a different type of polymers. And the pressure inside the bubble $\bar{p}_g$ in the equation (1.10) is calculated similarly to that of Patel and Han and Yoo. However, in chapter two, the complete details are discussed on the formulation of $\bar{p}_g$ which depends on the concentration of gas in the liquid side.

The second part of their investigation is to compare the power-law model with the viscoelastic model. Ramesh et al. adopted the viscoelastic model developed by Arefmanesh and Advani (1990), which is based on Amon and Denson's (1984) cell model. Therefore, according to Ramesh, the noninertial momentum equation in the radial direction is given as

$$\bar{p}_g(t) - \bar{p}_a = \frac{2\sigma}{\bar{R}} - 2\int_{\bar{R}}^{\bar{S}} \frac{\bar{\tau}_{rr} - \bar{\tau}_{\theta\theta}}{\bar{r}}dr,$$ (1.11)

Here, $\bar{S}$ being the outer shell thickness of the bubble. The equation (1.11) requires the unknowns $\bar{p}_g(t)$, $\bar{\tau}_{rr}$ and $\bar{\tau}_{\theta\theta}$ to determine the bubble radius. Therefore as per Ramesh et al., the Arefmanesh and Advani's viscoelastic model that solves for the $\bar{\tau}_{rr}$ and $\bar{\tau}_{\theta\theta}$ are mathematically given as

$$\frac{d\bar{\tau}_{rr}}{d\bar{t}} + \left(\frac{1}{\lambda} + \frac{4\bar{R}^2\dot{\bar{R}}}{\bar{y} + \bar{R}^3} \right)\bar{\tau}_{rr} = -\frac{4\mu}{\lambda}\frac{\bar{R}^2\dot{\bar{R}}}{\bar{y} + \bar{R}^3}, \tag{1.12}$$

$$\frac{d\bar{\tau}_{\theta\theta}}{dt} + \left(\frac{1}{\lambda} - \frac{2\bar{R}^2\dot{\bar{R}}}{\bar{y} + \bar{R}^3} \right)\bar{\tau}_{\theta\theta} = \frac{2\mu}{\lambda}\frac{\bar{R}^2\dot{\bar{R}}}{\bar{y} + \bar{R}^3}. \tag{1.13}$$

Here, $\bar{y}$ represents the transformed coordinate in the Ramesh et al. formulation. Note that $\bar{p}_g(t)$ in the equation (1.11) is calculated in a similar method to that of the power-law model.

Ramesh et al.'s (1991) experimental and theoretical findings show that bubble growth depends on the type of blowing agent used, saturation pressure, the temperature, and the molecular weight of the gas. They insisted that the power-law and Newtonian law model underpredicts the bubble growth with experiments, however, they suggested that the viscoelastic model was slightly better in predicting the experimental results.

A lot of research has been carried out to understand the bubble dynamics in a supersaturated liquid, among them Elshereef, Vlachopoulos and Elkamel, (2010) compared two popular bubble growth models. The first model is known as Patel model or single bubble growth model which is developed on assumption that a single bubble grows in a pool of liquid with infinite availability of gas, and the second model is called a cell model or Amon and Denson model which is developed by incorporating the finiteness of gas availability and considering the proximity of gas bubbles.

The main motive of the Elshereef et al., (2010) investigation is to compare these two models in terms of numerical implementations and accuracy in bubble growth prediction.

In this regard, they compared the models with Han and Yoo's experimental findings. The non-inertial single gas bubble model (Patel's model) represented by Elshereef takes the form

$$\frac{d\bar{R}}{d\bar{t}} = \bar{R}\left(\frac{\bar{p}_g(t) - \bar{p}_a - 2\sigma/\bar{R}}{4\mu}\right). \tag{1.14}$$

For $\bar{p}_g(t)$ in the equation (1.1), the following explicit equation is represented by Elshereef. This equation is developed based on the thin boundary layer around the liquid. A detailed methodology for the derivation of this equation is stated in chapter two and is given as

$$\frac{d\bar{p}_g}{d\bar{t}} = \frac{6D\rho^2{}_L R^2{}_g T^2 k^2{}_h}{M^2}\left(\frac{\left(\bar{p}_{g0} - \bar{p}_g\right)^2 \bar{R}(t)}{\bar{p}_g(t)\bar{R}^3(t) - \bar{p}_{g0}\bar{R}_0{}^3}\right) - 3\bar{p}_g\left(\frac{\dot{\bar{R}}}{\bar{R}}\right), \tag{1.15}$$

with R_g being the universal gas constant, T being the temperature of the gas, k_h being Henry's law constant, M being the molecular weight of the gas, $\bar{p}_{g0}$ and $\bar{R}_0$ being the initial pressure inside the gas bubble and initial bubble radius.

Similarly, the second non-inertial bubble growth model (Amon and Denson Model) represented by Elshereef takes the form

$$\frac{d\bar{R}}{d\bar{t}} = \bar{R}\left(\frac{\bar{p}_g(t) - \bar{p}_a - 2\sigma/\bar{R}}{4\mu}\right)\left(\frac{\bar{S}^3(t)}{\bar{S}^3(t) - \bar{R}^3(t)}\right). \tag{1.16}$$

Here, $\overline{S}(t)$ is the instantaneous outer shell thickness. The equation to calculate the $\overline{S}(t)$ and pressure inside the bubble $\overline{p}_g(t)$ are given by R. Elshereef as

$$\overline{S}(t) = \left(\overline{S}_0^3 + R(t)^3 - \overline{R}_0^3 \right)^{1/3}, \tag{1.17}$$

Here $\overline{S}_0$ is the initial shell thickness,

$$\frac{d\overline{p}_g}{d\overline{t}} = \frac{3D\rho_L R_g T \overline{R}^2(t)}{M} \left(\frac{d\overline{c}}{d\overline{r}} \right)_{\overline{r}=\overline{R}} - 3\overline{p}_g \left(\frac{\dot{\overline{R}}}{\overline{R}} \right). \tag{1.18}$$

In equation (1.18), Elshereef calculated the gradient at the interface by solving the advection-diffusion equation numerically. However, the author lacks in providing a clear methodology of solving the equation numerically and the study of diffusion in the vicinity of the bubble is ignored.

For a better understanding, the important models are tabulated as shown in the table (1-1). The overview of the models is presented based on the solution procedure of the advection-diffusion equation, the type of fluid used, and based on confinement of the bubbles.

Table 1-1: Assumptions made in the different models

Model	Liquid	Solving Diffusion equation	Availability of experimental data	Availability of gas in the liquid	Bubble confinement
Model 1 -Patel 1980	Newtonian	Boundary layer assumption to get the approximated	No	infinite	No

		solution to the diffusion equation			
Model 2 - Amon and Denson 1984	Newtonian	Numerical	No	finite	yes
Han and Yoo 1981	Viscoelastic	Boundary layer assumption to get the approximated solution to the diffusion equation and also presented the viscoelastic effect in the model	yes	infinite	No
Present model	Newtonian	Numerical	No	infinite	No

1.6 Research Gaps

Although researchers have done ample work in understanding the hydrodynamics of the bubbles in different processes, a clear insight into the diffusion process and explanation of numerical procedures are lacking. The current work emphasizes solving the diffusion process numerically and studying the different flow parameters affecting the hydrodynamics of bubble growth. The current thesis also focuses on comparing the present

work with the different models Elshereef eta al. (2010) and experimental data of Han and Yoo.

1.7 Thesis Outline

In the second chapter, a detailed mathematical model will be developed that describes the hydrodynamics of bubbles from the fundamentals of mass and momentum equations. Thereafter, an approximate solution to the advection-diffusion equation that is extensively used in the literature is rederived. The present developed model is non-dimensionalized using appropriate scales and finally, a detailed numerical approach to the developed model will be discussed.

Chapter three is dedicated to results and discussions. Where we start by validating the present numerical approach by reproducing the noninertial growth results of Elshereef et al., (2010). Then we discuss the results obtained by adding inertia into their formulation. Thereafter, the approximated analytical solution to the advection-diffusion equation is compared with the present numerical model, followed by comparisons of the present numerical model with available theory and experiments. The second part of chapter three will be focused on the parametric study, which includes the study of viscosity, surface tension, system pressure, Henry's constant, and diffusion coefficient effects on the bubble growth.

The final chapter of the thesis will present the conclusions and briefs on future developments that can be done on the existing work.

Chapter 2

2 Governing Equations of Bubble Growth

The hydrodynamics of an isolated spherically symmetrical gas bubble whose radius is $\bar{R}(\bar{t})$ in an incompressible gas-liquid solution is described by the conservation of mass and momentum equations.

The problem is modeled in spherical ($\bar{r}, \theta, \phi$) space. The growth of the bubble is induced by the pressure and concentration gradients. It is assumed that the partial pressure of the gas at infinity (far away from the bubble) is constant and equal to an equilibrium pressure $\bar{p}_0$. The pressure $\bar{p}_R(t)$ and $\bar{p}_g(t)$ are the pressures experienced at the interface and inside the gas bubble respectively. $\bar{c}(r,t)$ being the concentration of gas in the liquid at a given time and position. The equilibrium concentration of the gas in the solution is denoted as $\bar{c}_0$, whereas the concentration at the interface of the bubble is $\bar{c}_R(t)$. Figure (2-1) represents the schematic view of the problem, note that the terms interface velocity and fluid velocity will be introduced with their definitions in the subsequent sections of the current chapter.
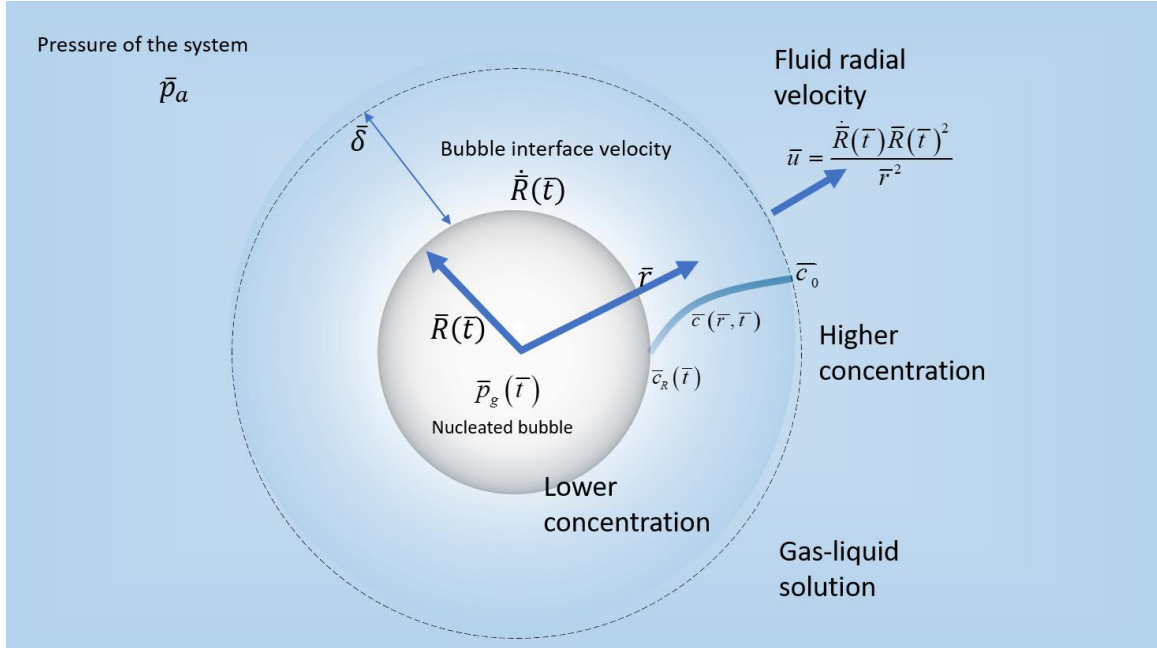
Figure 2-1: Schematic diagram of a single bubble in a liquid-gas solution

2.1 Conservation of Mass

Let $\bar{u}_\theta$, $\bar{u}_\phi$ and $\bar{u}_r$ be the velocity components in the spherical $\bar{r}$, θ and ϕ space. Let $\bar{r}$

be any radial position from the center of the bubble., The general continuity equation in

spherical coordinates for Newtonian liquid of density ρ_L takes the form

$$\frac{\partial \rho_L}{\partial \bar{t}} + \rho_L \left(\frac{1}{\bar{r}^2} \frac{\partial}{\partial \bar{r}} \left(\bar{r}^2 \bar{u}_r \right) + \frac{1}{\bar{r}\sin\theta} \frac{\partial}{\partial \theta} \left(\sin\theta \bar{u}_\theta \right) + \frac{1}{\bar{r}\sin\theta} \frac{\partial \bar{u}_\phi}{\partial \phi} \right) = 0. \tag{2.1}$$

Assuming that the bubble changes its dimension only in the radial direction $\bar{r}$, the non-

radial velocity components $\bar{u}_\theta$ and $\bar{u}_\phi$ are neglected. Therefore, for an incompressible

liquid, the equation (2.1) takes the final form

$$\frac{1}{\bar{r}^2} \frac{\partial}{\partial \bar{r}} \left(\bar{r}^2 \bar{u}_r \right) = 0. \tag{2.2}$$

2.1.1 Kinematic Boundary Condition

The kinematic boundary condition states that the difference in normal velocities of the fluid particle and the moving surface which are in contact equals to zero. In this case, let the velocity of the fluid particle at the interface is $\bar{u}_R$ and the velocity of the bubble surface is the rate of change of bubble radius $\dfrac{d\bar{R}}{d\bar{t}}$ (see figure 2-1). Therefore, the kinematic boundary condition at the interface takes the form

$$\bar{u}_R = \frac{d\bar{R}}{d\bar{t}}. \tag{2.3}$$

2.1.2 Fluid Velocity

For convenience, the radial component of velocity $\bar{u}_r$ will now simply be written as $\bar{u}$ and differentiation is represented by a dot.

To find the expression for the radial velocity $\bar{u}$ one can immediately integrate equation (2.2) in the radial direction and get the equation

$$\bar{u} = \frac{f(t)}{\bar{r}^2}. \tag{2.4}$$

The time-dependent function in the equation of velocity (2.4) can be obtained by applying the kinematic boundary condition (2.3), which results in

$$f(t) = \dot{\bar{R}}\bar{R}^2, \tag{2.5}$$

by substituting equation (2.5) in (2.4) yields to the expression for radial velocity, in terms of bubble growth rate, its radius, and position (see figure 2-1)

$$\bar{u} = \frac{\dot{\bar{R}}\bar{R}^2}{\bar{r}^2}.$$
(2.6)

2.2 Conservation of Momentum

The radial motion of the fluid can be described by the radial momentum equation. Gravity does not paly much importance in the analysis, therefore, the conservation of momentum equation in terms of pressure and stress without the gravitational force is expressed as

$$\rho_L \left(\frac{\partial \bar{u}}{\partial \bar{t}} + \bar{u} \frac{\partial \bar{u}}{\partial \bar{r}} \right) = -\frac{\partial \bar{p}}{\partial \bar{r}} + \frac{\partial \bar{\tau}_{rr}}{\partial \bar{r}} + \frac{2\bar{\tau}_{rr}}{r} - \frac{\bar{\tau}_{\theta\theta} + \bar{\tau}_{\phi\phi}}{r},$$
(2.7)

where $\bar{\tau}_{rr}, \bar{\tau}_{\theta\theta}, \bar{\tau}_{\phi\phi}$ are the non-zero normal stress components of the stress tensor in radial, angular, and azimuthal directions respectively, and $\bar{p}$ is the pressure.

knowing the fact that some of the diagonal components of a stress tensor are zero (Fogler and Goddard, 1970) ($\bar{\tau}_{rr} + \bar{\tau}_{\theta\theta} + \bar{\tau}_{\phi\phi} = 0$), we can express $\bar{\tau}_{\theta\theta} + \bar{\tau}_{\phi\phi}$ in terms of $\bar{\tau}_{rr}$, or by spherical symmetricity, we can express $\bar{\tau}_{\theta\theta}$ in terms of $\bar{\tau}_{\phi\phi}$ as $\bar{\tau}_{\theta\theta} = \bar{\tau}_{\phi\phi}$ (Han and Yoo, 1981). Both assumptions result in the same results. In the next section, we apply spherical symmetricity to the equation (2.7) and see that in the resulting equation, viscosity vanishes after replacing the velocity in terms of bubble growth rate and its radius in the equation.

2.2.1 Spherical Symmetricity of the Bubble

According to Han and Yoo, (1981), applying spherical symmetricity i.e. $\overline{\tau}_{\theta\theta} = \overline{\tau}_{\phi\phi}$ to the momentum equation (2.7) results in

$$\rho_L \left(\frac{\partial \overline{u}}{\partial \overline{t}} + \overline{u} \frac{\partial \overline{u}}{\partial \overline{r}} \right) = -\frac{\partial \overline{p}}{\partial \overline{r}} + \frac{\partial \overline{\tau}_{rr}}{\partial \overline{r}} + \frac{2\overline{\tau}_{rr}}{r} - \frac{2\overline{\tau}_{\theta\theta}}{\overline{r}} , \qquad (2.8)$$

We can replace $\overline{\tau}_{rr}$ and $\overline{\tau}_{\theta\theta}$ in equation (2.8) by using the definition of stress. For a Newtonian fluid normal stress equals to the viscosity of the liquid μ multiplied by its velocity gradient and given as

$$\overline{\tau}_{rr} = 2\mu \frac{\partial \overline{u}}{\partial \overline{r}} , \qquad (2.9)$$

$$\overline{\tau}_{\theta\theta} = \overline{\tau}_{\phi\phi} = 2\mu \frac{\overline{u}}{r} , \qquad (2.10)$$

replacing $\overline{\tau}_{rr}$ and $\overline{\tau}_{\theta\theta}$ with equation (2.9) and (2.10) in (2.8) results in the following form of momentum equation.

$$\rho_L \left(\frac{\partial \overline{u}}{\partial \overline{t}} + \overline{u} \frac{\partial \overline{u}}{\partial \overline{r}} \right) = -\frac{\partial \overline{p}}{\partial \overline{r}} + 2\mu \left(\frac{\partial^2 \overline{u}}{\partial \overline{r}^2} + \frac{2}{r} \frac{\partial \overline{u}}{\partial \overline{r}} - \frac{2\overline{u}}{r^2} \right) \qquad (2.11)$$

Form the expression of velocity (2.6), one can differentiate the partial derivatives of $\overline{u}$ with respect to time and position and yields the following equations

$$\frac{\partial \overline{u}}{\partial \overline{t}} = \frac{1}{\overline{r}^2} \ddot{\overline{R}}\overline{R}^2 + \frac{2\overline{R}}{\overline{r}^2} \dot{\overline{R}}^2 , \qquad (2.12)$$

$$\frac{\partial \overline{u}}{\partial \overline{r}} = \frac{-2\dot{\overline{R}}\overline{R}^2}{\overline{r}^3} \, , \tag{2.13}$$

$$\frac{\partial^2 \overline{u}}{\partial \overline{r}^2} = \frac{6\dot{\overline{R}}\overline{R}^2}{\overline{r}^4} \, , \tag{2.14}$$

by substituting equations (2.12) -(2.14) in equation (2.11) one can obtain the following equation, without the viscous term

$$\rho_L \left(\frac{\ddot{\overline{R}}\overline{R}^2}{\overline{r}^2} + \frac{2\dot{\overline{R}}^2\overline{R}}{\overline{r}^2} + \frac{-2\dot{\overline{R}}^2\overline{R}^4}{\overline{r}^5} \right) = -\frac{\partial \overline{p}}{\partial \overline{r}} \, . \tag{2.15}$$

The equation (2.15) is also true for the condition of Fogler and Goddard, (1970) which says the diagonal components of a stress tensor equal to zero ($\overline{\tau}_{rr} + \overline{\tau}_{\theta\theta} + \overline{\tau}_{\phi\phi} = 0$). The final form of the equation which describes the hydrodynamics of the bubble can be obtained by integrating equation (2.15) with respect to $\overline{r}$ from bubble interface $\overline{R}$ to infinity ∞ and by rearranging the terms yields to

$$\rho_L \left(\ddot{\overline{R}}\overline{R} + \frac{3}{2}\dot{\overline{R}}^2 \right) = \overline{p}_R - \overline{p}_a , \tag{2.16}$$

note that the pressure at infinity ∞ is the surrounding pressure of the liquid and is equal to $\overline{p}_a$ and is called as system pressure. The system could be anything starting from a beverage bottle to mold in the injection pressure foaming process.

2.2.2 Dynamic Condition

Let $\ddot{T}_R$ be the stress tensor in the liquid side, $\ddot{T}_g$ be the stress tensor on the gas side of the interface, and let σ , $\vec{n}$ are the surface tension in the liquid and the unit normal vector. The dynamic boundary condition states that stress at the interface has to be continuous., Mathematically the normal stress balance across the interface is represented as

$$\vec{n} \cdot \left(\ddot{T}_R - \ddot{T}_g \right) = \sigma \vec{n} \left(\nabla \cdot \vec{n} \right) \quad . \tag{2.17}$$

When a vector is dotted with the tensor, the resultant would be the vector, therefore from the equation (2.17) the normal vector dotted with tensor will give the normal force vector as follows.

Therefore, for the liquid side it is written as

$$\vec{n} \cdot \ddot{T}_R = -\bar{p}_R + \bar{\tau}_{rrR} , \tag{2.18}$$

Similarly, for the gas side it is given as

$$\vec{n} \cdot \ddot{T}_g = -\bar{p}_g + \bar{\tau}_{rrg} . \tag{2.19}$$

And the divergence of the normal vector is related to the mean curvature of the interface, which takes the form.

$$\nabla \cdot \vec{n} = \frac{2}{R} . \tag{2.20}$$

Here $\bar{\tau}_{rrR}$ is the normal stress component at the interface in the liquid side and $\bar{\tau}_{rrg}$ is the normal stress component in the gas side (see figure (2-2)).
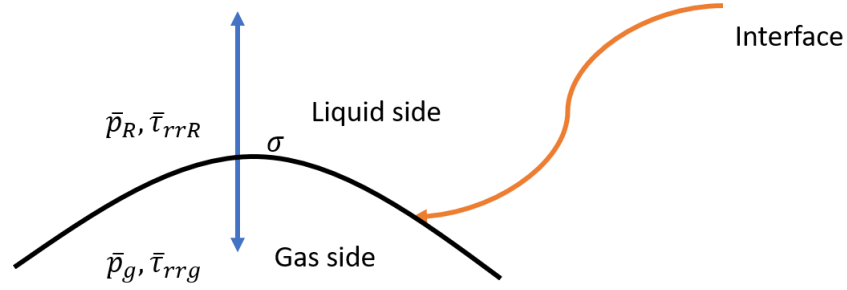
Figure 2-2: Dynamic condition at the interface

Assuming that the effect of normal stress on the gas side is zero i.e $\overline{\tau}_{rrg} = 0$ and

substituting equation (2.18)-(2.20) in (2.17) and replacing the partial derivative of $\overline{\tau}_{rrR}$

with bubble radius and its velocity (2.6) results in the following condition

$$\overline{p}_g = \frac{2\sigma}{\overline{R}} + \overline{p}_R + \frac{4\mu\dot{\overline{R}}}{\overline{R}}, \tag{2.21}$$

from equation (2.21) $\overline{p}_R$ can be substituted in equation (2.16) which results in

$$\rho_L\left(\ddot{\overline{R}}\overline{R} + \frac{3}{2}\dot{\overline{R}}^2\right) = \overline{p}_g - \frac{2\sigma}{\overline{R}} - \frac{4\mu\dot{\overline{R}}}{\overline{R}} - \overline{p}_a. \tag{2.22}$$

Equation (2.22) is called as a Rayleigh-Plesset hydrodynamics equation for bubble growth

inside a liquid whose viscosity is μ and surface tension is σ. Here, the growth of the

bubble is dictated by pressure difference $\overline{p}_g - \overline{p}_a$ where $\overline{p}_g > \overline{p}_a$.

2.3 Bubble Growth due to Mass Transfer

In a supersaturated liquid, bubbles grow due to diffusive mass transfer across its interface from its surroundings. Therefore, one can say that the mass flux diffusing across the interface is equal to the rate of change of mass inside the gas bubble.

Let the mass of the gas at the interface is m_R, according to Fick's first law, the mass flux at the interface of a spherical bubble has the value

$$\dot{m}_R = 4\pi \bar{R}^2 \rho_L D \left(\frac{\partial \bar{c}}{\partial \bar{r}} \right)_{\bar{R}},$$ (2.23)

here, $\left(\dfrac{\partial \bar{c}}{\partial \bar{r}} \right)_{\bar{R}}$ is the concentration gradient of the gas at the interface and D is the diffusion coefficient of the gas-liquid solution.

Similarly, let the mass of the gas inside the bubble be m_g and its density be ρ_g. Then the rate of change of mass inside the spherical bubble whose volume is $V_g = \dfrac{4}{3}\pi \bar{R}^3$ has the value

$$\frac{dm_g}{d\bar{t}} = 4\pi \bar{R}^2 \left(\rho_g \dot{\bar{R}} + \frac{\bar{R}}{3} \dot{\rho}_g \right),$$ (2.24)

assuming, that the gas inside the bubble follows ideal gas law, the density of the gas (ρ_g) in the bubble can be replaced with pressure ($\bar{p}_g$), which is given as

$$\rho_g = \frac{\bar{p}_g M}{R_g T}.$$ (2.25)

Here R_g is the universal gas constant, T is the temperature of the gas and M is the molar gas weight. Substitution of equation (2.25) in equation (2.24) yields to

$$\frac{dm_g}{d\bar{t}} = \frac{1}{R_g T} 4\pi \bar{R}^2 \left(\bar{p}_g \dot{\bar{R}} + \frac{\bar{R}}{3} \dot{\bar{p}}_g \right). \tag{2.26}$$

Now by applying the conservation of mass at the interface i.e., $\dot{m}_R = \dfrac{dm_g}{dt}$, one can get the expression for the variation of pressure with time inside the gas bubble as follows

$$\frac{d\bar{p}_g}{dt} = \frac{R_g T \rho_L D}{M} \frac{3}{\bar{R}} \left(\frac{\partial \bar{c}}{\partial \bar{r}} \right)_{\bar{R}} - 3\bar{p}_g \left(\frac{\dot{\bar{R}}}{\bar{R}} \right). \tag{2.27}$$

Equation (2.22) and (2.27) can be coupled and solved simultaneously for the bubble growth and pressure variation inside the bubble. However, to solve the equation (2.27) one has to know the concentration gradient at the interface, therefore in the next section, a scalar advection-diffusion equation is introduced.

2.3.1 Advection-Diffusion Equation

The concentration of gas in the liquid $\bar{c}\left(\bar{r},\bar{t}\right)$ can be described by the scalar transport advection-diffusion equation which is given as

$$\frac{\partial \bar{c}}{\partial \bar{t}} + \bar{u} \frac{\partial \bar{c}}{\partial \bar{r}} = D \left(\frac{2}{\bar{r}} \frac{\partial \bar{c}}{\partial \bar{r}} + \frac{\partial^2 \bar{c}}{\partial \bar{r}^2} \right), \tag{2.28}$$

here, $\bar{u}$ can be replaced in terms of bubble radius and interface velocity using equation (2.8), and this way equation (2.28) is also coupled with a hydrodynamic equation and can be written as

$$\frac{\partial \overline{c}}{\partial \overline{t}} + \frac{\dot{\overline{R}}\overline{R}^2}{\overline{r}^2} \frac{\partial \overline{c}}{\partial \overline{r}} = D\left(\frac{2}{\overline{r}} \frac{\partial \overline{c}}{\partial \overline{r}} + \frac{\partial^2 \overline{c}}{\partial \overline{r}^2} \right),$$
(2.29)

the coupled Equations (2.22), (2.27), and (2.29) need to be solved simultaneously to get the bubble growth, pressure variation inside the bubble, and concentration of gas in the liquid.

Equation (2.27) is similar to the equation (50) in the Elshereef et al. 2010 formulation. However, he used an approximate analytical solution to the equation (2.29) to calculate the concentration gradient that appears in equation (2.27). The approximate solution was originally derived by Patel, (1980) using a thin boundary layer approach, which is going to be discussed later in the following sections. In this thesis, one of the main goals is to solve the (2.29) equation numerically using a finite difference approach and compare it with the approximated analytical results.

The boundary and initial conditions to the equation (2.29) are related to the concept of Henry's law, therefore, in the immediate next section, a detailed explanation is given to the concept of Henry's law.

2.3.2 Henry's law

For diffusive growth bubbles, the pressure at the interface is always in thermodynamic equilibrium with the pressure inside the gas bubble. This equilibrium relation can be described using Henry's law.

Henry's law states that at constant temperature T, the equilibrium concentration, $\overline{c}$, of dissolved gas in a liquid is directly proportional to its partial pressure $\overline{p}$, multiplied with a constant known as Henry's constant. Mathematically it is given as

$$\overline{c} = k_h(T)\overline{p}. \tag{2.30}$$

Where k_h is Henry's constant and it is a constant for a given liquid-gas solution

2.4 Initial and Boundary Conditions

Equation (2.22) is a non-linear second-order ordinary differential equation in time; therefore, it requires two initial conditions. The first initial condition comes from the assumption that that the bubble is nucleated prior and has an initial finite radius $\overline{R}_0$ and for the second initial condition, it is assumed that, initially the interface of the bubble is at rest. Therefore, the two initial conditions associated with equation (2.22) are written as

$$\overline{R}(\overline{t} = 0) = \overline{R}_0, \tag{2.31}$$

$$\dot{\overline{R}}(\overline{t} = 0) = 0. \qquad . \tag{2.32}$$

Similarly, equation (2.27) requires an initial condition to solve for the pressure variation inside the bubble and it originates from the thermodynamic equilibrium at the interface. It is assumed that after the nucleation, the pressure inside the bubble is in equilibrium with the initial saturation pressure $\overline{p}_{g0}$ and given as

$$\overline{p}_g(0) = \overline{p}_{g0}. \tag{2.33}$$

The initial condition for the equation (2.29) comes from the assumption that, after the nucleation of the bubble, concentration is uniformly distributed in the liquid and it is equal to the dissolved concentration $\overline{c}_0$. Therefore, it is written as

$$\overline{c}\left(\overline{r},0\right)=\overline{c}_0. \tag{2.34}$$

The remaining two boundary conditions for the equation (2.29) are the equilibrium condition of the concentration at the interface, which is described by Henry's law, and the concentration far away from the bubble which is assumed to be equal to the saturation concentration

$$\overline{c}\left(\overline{r}=\overline{R},\overline{t}\right)=\overline{c}_R\left(\overline{t}\right)=k_h\overline{p}_g\left(\overline{t}\right), \tag{2.35}$$

$$\overline{c}\left(\overline{r}=\infty,\overline{t}\right)=\overline{c}_0. \tag{2.36}$$

2.5 Concentration Gradient Approximation at the Interface

The approximate parabolic concentration profile assumed by Rosner and Epstein, (1972) to the diffusion equation (2.29) is very well known in the literature for the diffusive bubble growth problems. This profile is used by several authors starting from Patel, (1980), Han and Yoo, (1981) to Elshereef et al. (2010) to determine the approximate solution to the diffusion equation. To appreciate and see the physical significance of parameters, the approximated solution of Patel (1980) is rederived in this section with the concentration profile assumption by Rosner and Epstein (1972).

Patel (1980) assumed a very thin boundary layer $\delta\left(\bar{t}\right)$ (see figure (2-3)) that changes with the time and also assumed a parabolic concentration profile of Rosner and Epstein (1972) in the boundary layer region and given as

$$\bar{c}\left(\bar{r},\bar{t}\right)=\bar{c}_0-\left(\bar{c}_0-\bar{c}_R\right)\left(1-\frac{\bar{r}-\bar{R}\left(\bar{t}\right)}{\bar{\delta}\left(\bar{t}\right)}\right)^2.$$ (2.37)
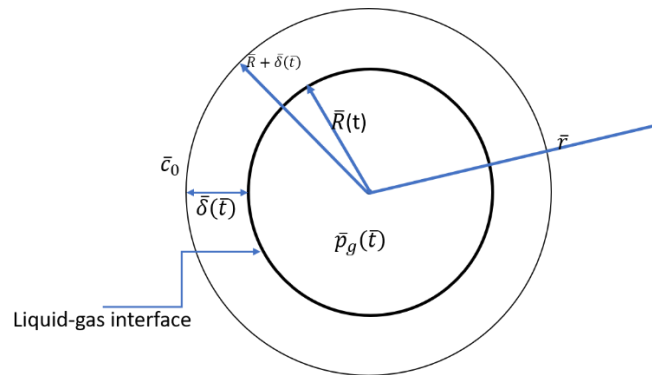

Figure 2-3: Boundary layer around a bubble

To get the concentration gradient at the interface, one can differentiate equation (2.37) with respect to r and evaluate the derivative at r = R and get the equation

$$\left(\frac{\partial\bar{c}}{\partial\bar{r}}\right)_{\bar{r}=\bar{R}}=\frac{2\left(\bar{c}_0-\bar{c}_R\right)}{\bar{\delta}\left(\bar{t}\right)}.$$ (2.38)

In the equation (2.38), Patel approximated $\bar{\delta}\left(\bar{t}\right)$ by integrating the diffusion equation from $\bar{R}$ to $\bar{R}+\bar{\delta}\left(\bar{t}\right)$ with the help of conservation of mass at the interface and assumed

parabolic concentration profile. He also assumed that $\left(\dfrac{\bar{\delta}(\bar{t})}{\bar{R}} \ll 1\right)$ which made him

drop the terms that are the order $O\left(\dfrac{\bar{\delta}(\bar{t})}{\bar{R}}\right)^2$ and arrived the equation for the boundary

layer $\bar{\delta}(\bar{t})$ which is given as

$$\bar{\delta}(\bar{t}) = \frac{M}{\rho_L R_g T}\left(\frac{\bar{p}_g(t)\bar{R}^3(t) - \bar{p}_{g0}\bar{R}_0^3}{(\bar{c}_0 - \bar{c}_R)\bar{R}^2(t)}\right). \tag{2.39}$$

One can substitute the boundary layer thickness equation (2.39) into equation (2.38) and can obtain the equation for concentration gradient at the interface, which is in terms of bubble gas pressure, bubble radius, and concentration

$$\left(\frac{\partial \bar{c}}{\partial \bar{r}}\right)_{\bar{r}=\bar{R}} = \frac{\rho_L R_g T}{M}\frac{2(\bar{c}_0 - \bar{c}_R)^2\,\bar{R}^2(t)}{\bar{p}_g(t)\bar{R}^3(t) - \bar{p}_{g0}\bar{R}_0^3}, \tag{2.40}$$

substitution of equation (2.40) in the (2.27) to yields to

$$\frac{d\bar{p}_g}{d\bar{t}} = \frac{6D\rho_L^2 R_g^2 T^2}{M^2}\left(\frac{(\bar{c}_0 - \bar{c}_R)^2\,\bar{R}(t)}{\bar{p}_g(t)\bar{R}^3(t) - \bar{p}_{g0}\bar{R}_0^3}\right) - 3\bar{p}_g\left(\frac{\dot{\bar{R}}}{\bar{R}}\right). \tag{2.41}$$

To make the equation (2.41) in terms of pressure, the initial dissolved concentration and concentration at the interface are replaced with initial pressure and pressure inside the bubble, which yields to the following first-order Ordinary differential equation

$$\frac{d\bar{p}_g}{d\bar{t}} = \frac{6D\rho_L^2 R_g^2 T^2 k_h^2}{M^2}\left(\frac{(\bar{p}_{g0} - \bar{p}_g)^2\,\bar{R}(t)}{\bar{p}_g(t)\bar{R}^3(t) - \bar{p}_{g0}\bar{R}_0^3}\right) - 3\bar{p}_g\left(\frac{\dot{\bar{R}}}{\bar{R}}\right). \tag{2.42}$$

Equation (2.42) is the same equation (50) in Elshereef, Vlachopoulos and Elkamel, (2010), but in the equation (2.42) there is $\bar{R}(t)$ appearing in the numerator, whereas in the Elshereef et al. (2010), it is missing. However, equation (2.42) is dimensionally correct and the missing $\bar{R}(t)$ in Elshereef et al. (2010) is considered as typing mistake.

One can solve the coupled equations (2.22) and (2.42) simultaneously for the bubble growth and pressure variation inside the bubble subjected to the initial conditions (2.31) to (2.33).

2.6 Domain Mapping

The interface of the bubble changes with time which makes the numerical procedure for solving the concentration distribution in the liquid more complicated and time-consuming. One of the methods which track the interface of the bubble with time is to re-mesh the computational domain at each time step, which not only costs computational time but also leads to computational errors.

An effective way to tackle this problem is to transform the coordinate such that the interface in the transformed coordinate is fixed. Therefore, the new coordinate is written as

$$\bar{x}(\bar{r},\bar{t}) = \bar{r} - \bar{R}(t). \tag{2.43}$$

With the help of equation (2.43), the partial derivatives in the advection-diffusion equation are changed from r to new coordinate x as

$$\frac{\partial \bar{c}}{\partial \bar{r}} = \frac{\partial \bar{c}}{\partial \bar{x}}, \tag{2.44}$$

$$\frac{\partial^2 \overline{c}}{\partial \overline{r}^2} = \frac{\partial^2 \overline{c}}{\partial \overline{x}^2}, \tag{2.45}$$

$$\frac{\partial \overline{c}}{\partial \overline{t}} = \frac{\partial \overline{c}}{\partial \overline{t}} - \frac{\partial \overline{c}}{\partial \overline{x}} \dot{R}. \tag{2.46}$$

Substituting in the equations (2.43-2.46) in (2.29) yield to

$$\frac{\partial \overline{c}}{\partial \overline{t}} + \frac{\partial \overline{c}}{\partial \overline{x}} \left(\frac{\dot{R}\overline{R}^2}{\left(\overline{x}+\overline{R}\right)^2} - \dot{R} \right) = D \left(\frac{2}{\left(\overline{x}+\overline{R}\right)} \frac{\partial \overline{c}}{\partial \overline{x}} + \frac{\partial^2 \overline{c}}{\partial \overline{x}^2} \right). \tag{2.47}$$

Similarly, the transformed equation (2.27) which describes the variation of pressure inside the gas bubble and the boundary conditions written as

$$\frac{d\overline{p}_g}{dt} = \frac{R_g T \rho_L D}{M} \frac{3}{\overline{R}} \left(\frac{\partial \overline{c}}{\partial x} \right)_{x=0} - 3\overline{p}_g \left(\frac{\dot{R}}{\overline{R}} \right), \tag{2.48}$$

$$\overline{c}\left(x,0\right) = \overline{c}_0, \tag{2.49}$$

$$\overline{c}\left(x=0,\overline{t}\right) = \overline{c}_R\left(\overline{t}\right) = k_h \overline{p}_g\left(\overline{t}\right), \tag{2.50}$$

$$\overline{c}\left(x=\infty,\overline{t}\right) = \overline{c}_0. \tag{2.51}$$

2.7 Problem Non-Dimensionalization

It is convenient to use the non-dimensional form of equations rather than dimensional form. Non-dimensional form of equations will give insights to the magnitude of a group of physical parameters, which will help to see which physical parameter dominates than others.

Here the velocity is scaled with the characteristic velocity whose magnitude is

$$\sqrt{\frac{\left(\bar{p}_{g0} - \bar{p}_a\right)}{\bar{\rho}_L}}$$, the radial position and the bubble radius is scaled with an initial bubble

radius $\bar{R}_0$ and it is convenient to scale the concentration with equilibrium concentration $\bar{c}_0$

. And the time is scaled with the reference time scale whose magnitude is the ratio of initial

bubble radius to characteristic velocity $t_{ref} = \dfrac{\bar{R}_0}{\bar{V}}$. Note that the nondimensional quantities

are represented by dropping the bar on it and are mathematically given as

$$r = \frac{\bar{r}}{\bar{R}_0} \quad , \quad c = \frac{\bar{c}}{\bar{c}_0}, \quad t = \frac{\bar{t}}{t_{ref}}, \quad R = \frac{\bar{R}}{\bar{R}_0}, \quad p = \frac{\bar{p}}{\bar{p}_{g0}}. \tag{2.52}$$

After rescaling the governing equations there are five non-dimensional groups, three of

these are the familiar Reynolds number Re, capillary number Ca, and Peclet number Pe

and their definitions are given as

$$\text{Re} = \frac{\rho_L V R_0}{\mu_L} \quad , \quad Ca = \frac{\rho_L \bar{V}^2 R_0}{\sigma}, \quad Pe = \frac{V \bar{R}_0}{D}. \tag{2.53a-c}$$

The additional two new non-dimensional numbers are named as Z and I , which take

the forms

$$Z = \frac{\bar{p}_{g0}}{\bar{V}^2 \rho_L}, \text{ and } I = \frac{\rho_L R_g T k_h}{M}. \tag{2.54a-b}$$

Here Reynolds weighs between the inertia of the liquid to its viscosity and on the other

hand, capillary number assesses between the surface tension and inertia of the liquid,

whereas the Peclet number competes between the convective mass transfer and diffusive mass transfer. The new number Z balance between the saturation pressure and inertia of the liquid and finally the non-dimensional number I compares between the solubility of the gas to its molecular weight.

Therefore, the momentum equation (2.22) after scaling is written as

$$\ddot{R}R + \frac{3}{2}\dot{R}^2 = Z\left(p_g - p_a\right) - \frac{2}{RCa} - \frac{4\dot{R}}{R\,\mathrm{Re}}. \tag{2.55}$$

Similarly, equation (2.48) and (2.42) which describes the pressure variation in the bubble takes the form

$$\frac{dp_g}{dt} = \frac{3I}{RPe}\left(\frac{\partial c}{\partial x}\right)_{x=0} - 3p_g\left(\frac{\dot{R}}{R}\right), \tag{2.56}$$

$$\frac{dp_g}{dt} = \frac{6I^2}{Pe}\left[\frac{\left(p_{g0} - p_g\right)^2 R}{\left(p_g R - p_{g0}R_0^{\,3}\right)}\right] - 3p_g\left(\frac{\dot{R}}{R}\right). \tag{2.57}$$

And finally, the scalar diffusion equation (2.47) is scaled and takes the form

$$\frac{\partial c}{\partial t} + \frac{\partial c}{\partial x}\left(\frac{\dot{R}R^2}{\left(x+R\right)^2} - \dot{R}\right) = \frac{1}{Pe}\left(\frac{2}{x+R}\frac{\partial c}{\partial x} + \frac{\partial^2 c}{\partial x^2}\right). \tag{2.58}$$

The rescaled boundary conditions subjected to (2.55), (2.56), and (2.58) are given as

$$R\left(t=0\right)=1, \tag{2.59}$$

$$\dot{R}\left(t=0\right)=0, \tag{2.60}$$

$$p_g(0)=1, \tag{2.61}$$

$$c(x,0)=1, \tag{2.62}$$

$$c(x=0,\mathrm{t})=c_R(t)=\frac{k_h \overline{p}_{g0}}{\overline{c}_0}p_g(t), \tag{2.63}$$

$$c(x=\infty,\mathrm{t})=1. \tag{2.64}$$

2.8 Numerical Implementation

The equation (2.55) is a non-linear second order ODE which describes the bubble growth. If the pressure in the bubble is constant, one can solve the equation (2.55) for the bubble growth $R(t)$ and its interface velocity $\dot{R}(t)$, with the use of any readily available numerical time integration solver like Ode45 in MATLAB. Ode45 is a nonstiff solver which uses Runge-Kutta 4th and 5th order to evaluate the future time derivative value. But the difficulty arises when the pressure inside the bubble varies with time, and it then needs to be coupled with the scalar diffusion equation to solve for the concentration gradient at the interface. Also, the scalar diffusion equation (2.58) contains a highly non-linear convective term in terms of bubble radius and its interface velocity. This combination makes the equations stiffer and requires a solution of the hydrodynamic equation (2.55), the pressure variation in the bubble (2.56), and the diffusion equation (2.58) simultaneously. Therefore, solving the highly stiff equation with Ode45 takes a very long time. Instead of Ode45, a variable order of accuracy solver Ode15s is used to integrate the equations. Here Ode15s uses 1st to 5th orders, it changes the orders as and when required and takes much less time compared to the Ode45 solver.

Now to solve these two equations simultaneously, the second-order hydrodynamic equation (2.55) primarily needs to be converted into the system of first-order ODE's by letting $R = y_1$. Therefore, the system of 1st order ODE's are given as,

$$\frac{dR}{dt} = y_2, \tag{2.65}$$

$$\frac{dy_2}{dt} = \frac{1}{y_1}\left(Z(p_g - p_a) - \frac{2}{y_1 Ca} - \frac{4y_2}{y_1 Re} - \frac{3}{2}y_2^2\right). \tag{2.66}$$

This way, when equation (2.66) is integrated one can get y_2, which is bubble interface velocity, and similarly equation (2.65) is integrated to get y_1 which is the bubble radius.

Since the equation (2.58) is partial in time and space, one can approximate either time or space using the finite difference methods. For convenience, the space partial derivative is approximated with finite-difference, up to the second-order accuracy.

Let i be the node position, and N be the total number of nodes (see figure (2-4)) in the gas-liquid solution starting from the interface x=0 to the infinity. The central difference scheme is adopted for the derivates. Therefore, the finite difference approximation for the first and second-order derivatives with central difference schemes are written as

$$\frac{\partial c}{\partial x} = \frac{c_{i+1} - c_{i-1}}{2dx}, \tag{2.67}$$

$$\frac{\partial^2 c}{\partial x^2} = \frac{c_{i+1} - 2c_i + c_{i-1}}{dx^2}. \tag{2.68}$$

The discretized form of the scalar diffusion equation using equations (2.67) and (2.68) takes the form

$$\frac{dc_i}{dt} = \frac{1}{Pe}\left(\frac{2}{(x_i+R)}\left(\frac{c_{i+1}-c_{i-1}}{2dx}\right)+\left(\frac{c_{i+1}-2c_i+c_{i-1}}{dx^2}\right)\right)-\left(\frac{c_{i+1}-c_{i-1}}{2dx}\right)\left(\frac{\dot{R}R^2}{(x_i+R)^2}-\dot{R}\right),$$

(2.69)

the discretized form of diffusion equation (2.69) needs to be solved at N-2 ($1 < i < N$) nodes starting from i=2 to i=N-1. Whereas at the interface, i.e. at i=1, the boundary condition (2.63) can be written in terms of ODE as

$$\frac{dc_1}{dt} = \left(\frac{k_h \bar{P}_{g0}}{\bar{c}_0}\right)\frac{dp_g}{dt},$$

(2.70)

And the final node serves as a boundary and the value of concentration is known from the boundary condition (2.64), therefore at i = N,

$$c_N = 1.$$

(2.71)
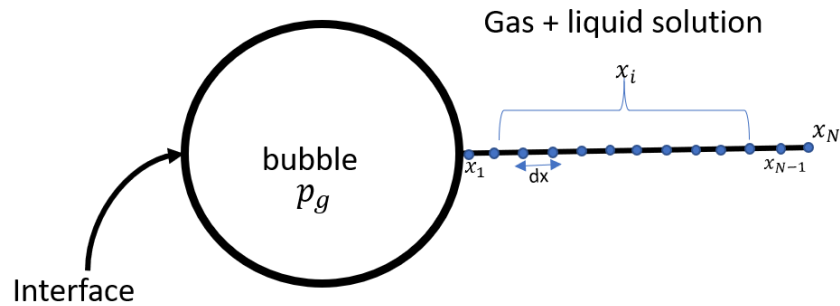
Figure 2-4: Numerical domain

Similarly, the concentration gradient at the interface in the equation (2.56) is discretized using the Forward finite difference scheme and is given as

$$\frac{\partial c}{\partial x} = \frac{c_{i+1} - c_i}{dx},$$

(2.72)

the substitution of equation (2.71) in (2.56) results in

$$\frac{dp_g}{dt} = \frac{3I}{RPe}\left(\frac{c_{i+1} - c_i}{dx}\right) - 3\overline{p}_g\left(\frac{\dot{R}}{R}\right).$$

(2.73)

To be consistent with the notation used for the hydrodynamic ODE's (2.65) to (2.66), the equations from (2.69) to (2.73) are rewritten in terms of y as follows.

Therefore equation (2.73) in terms of y takes the form

$$\frac{dy_3}{dt} = \frac{3I}{y_1 Pe}\left(\frac{y_5 - y_4}{dx}\right) - 3y_3\left(\frac{y_2}{y_1}\right).$$

(2.74)

Similarly, equations (2.69) to (2.71) are written as follows.

At the interface $(i = 1)$

$$\frac{dc_{y_3+i}}{dt} = \left(\frac{k_h \overline{P}_{g0}}{\overline{c}_0}\right)\frac{dy_3}{dt},$$

(2.75)

from node ($1 > i < N$),

$$\frac{dy_{3+i}}{dt} = \frac{1}{Pe}\left(\frac{2}{(x_i + y_1)}\left(\frac{y_{3+(i+1)} - y_{3+(i-1)}}{2dx}\right) + \left(\frac{y_{3+(i+1)} - 2y_{3+i} + y_{3+(i-1)}}{dx^2}\right)\right) - \left(\frac{y_{3+(i+1)} - y_{3+(i-1)}}{2dx}\right)\left(\frac{y_2 y_1^2}{(x_i + y_1)^2} - y_2\right)$$

(2.76)

and at the final boundary node $i = N$

$$y_{N+3} = 1. \tag{2.77}$$

Therefore, the total (N+3) equations starting from (2.65) to (2.66) and equations (2.74) to (2.76) are the final system of ODE's that are solved simultaneously subjected to the boundary conditions (2.59) to (2.64).

2.9 Summary

In summary, a mathematical model is developed from the governing mass and momentum equations in a spherical system. The spherical symmetricity to the bubble is applied and justified how viscosity initially vanishes in the hydrodynamic equations. The equation for the variation of pressure inside the bubble which couples with diffusion equation and hydrodynamic equations is developed from the interface mass transfer phenomenon. An analytical solution to the diffusion equation is rederived to understand the importance of hydrodynamic parameters.

The chapter is completed by introducing the nondimensional form of the developed equation and discussing the numerical procedure to solve the differential equations.

Chapter 3

3 Results and Discussion

This chapter starts by discussing the results obtained by the non-inertial bubble growth formulation presented by Elshereef et al., (2010) who used an approximate analytical solution to the diffusion equation developed by Patel (1980). Secondly, inertia is included in Elshereef et al. formulation and the results are compared with the non-inertial case. Thereafter, the results of the present developed numerical model are compared with experiments and existing theory, and finally, a detailed parametric study is carried out with the present developed bubble growth model.

3.1 Non-inertial Bubble Growth Model.

In this section, we start by reproducing the non-inertial bubble growth results from Elshereef et al. (2010). To do so we neglect inertia in the hydrodynamic equation (2.55) and use Patel's approximated concentration gradient (see equation (2.40)) in the equation (2.56). Therefore, after neglecting the left part (inertia) of equation (2.55), one can obtain the following first-order ordinary differential equation, which is presented as

$$\dot{R} = \frac{ZR\,\text{Re}}{4}\left(p_g - p_a\right) - \frac{\text{Re}}{2Ca}.$$

(3.1)

The non-dimensional equation (3.1) is equivalent to Elshereef et al. (2010) equation number (38). This equation along with the equation (2.57), which is similar to Elshereef et al. (2010) equation number (50) can be integrated with respect to time, subjected to initial

conditions (2.59) and (2.61) to get the instantaneous bubble growth and pressure variation inside the bubble.

Table 3-1: Flow parameters

Parameters	values
Type of gas in the bubble	CO_2
The molecular weight of the gas M	0.04401 kg/mol
Initial radius $\bar{R}_0$	10^{-6} m
Initial pressure inside the bulb $\bar{p}_{g0}$	4.7 atm
Ambient pressure $\bar{P}_a$	1.01 atm
Dynamic viscosity of the liquid μ_L	4000 Pa. s
The surface tension of the liquid σ	2.8×10^{-2} N/m
The density of the liquid ρ_L	880 kg/m^3
Ambient Temperature T	473 K
Henry's law constant k_h	4.26×10^{-9} m^2/N
Diffusion coefficient D	5.5×10^{-10} m^2/s

Since the equation (3.1) and (2.57) are in non-dimensional form, one can use the foaming process flow parameters presented by Elshereef et al. (2010) and Han and Yoo's (1981) (see table (3.1)) to calculate the non-dimensional numbers that appear in our equations. These are calculated as Re $=4.5\times10^{-6}$, Ca = 13.17, Z=1.27, I $=0.3$, and Pe= 3.7×10^{4}

respectively. It has been noticed that the equation (2.57) encounters singularity at t = 0, which creates initial complications in the numerical simulation. To avoid this problem the initial pressure (i.e. at t=0) p_{g0} is considered lesser than unity but almost close to unity (

$p_{g0}\ 0\ =0.9999\approx 1$).

The results reproduced using equation (3.1) and (2.57) match with the Elshereef et al., (2010) bubble radius data qualitatively and quantitatively (see Figure (3-1)). The non-dimensional interface velocity and pressure variation inside the gas bubble are shown in figures (3-2) and (3-3) respectively. From the plots, it is observed that the interface velocity of the bubble elevates to the peak in a short period and starts decreasing with time for the rest of bubble growth period, which indicates that the growth of the bubble is rapid at initial stages and decreases with time in the later stages. The same behavior can be observed from the pressure variation inside the bubble, where the pressure of the gas inside the bubble drops sharply at a small-time interval and remains nearly constant with time. This type of behavior suggests a diffusive dominant growth. However, due to the lack of results for the bubble interface velocity and bubble pressure variation in Elshereef et al., (2010), a comparison has not been made.
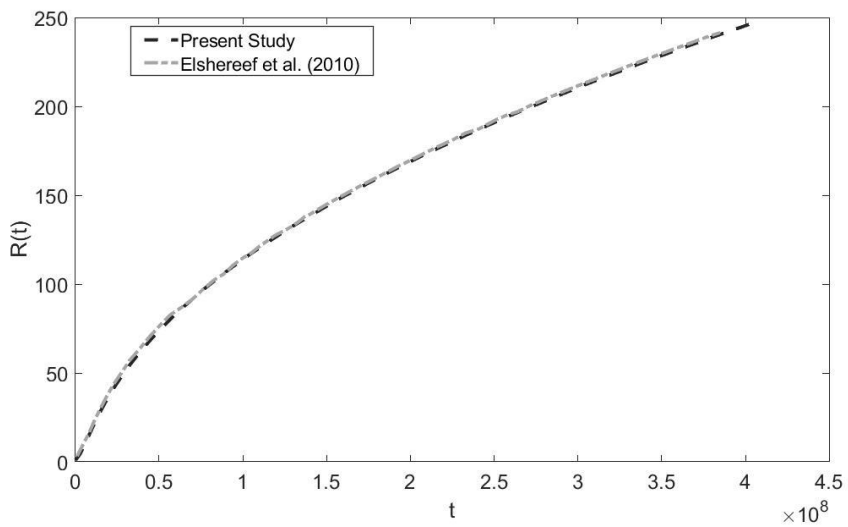
Figure 3-1: Bubble growth with time, reproduced results of Elshereef et al., (2010)
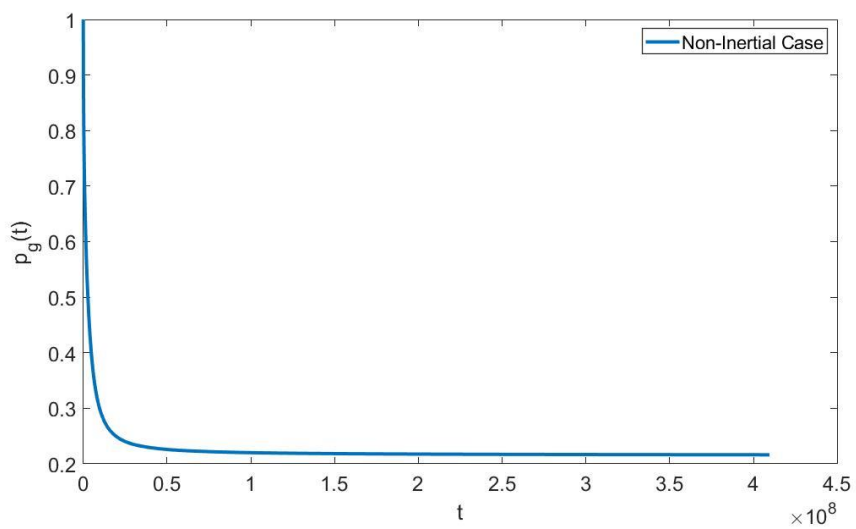
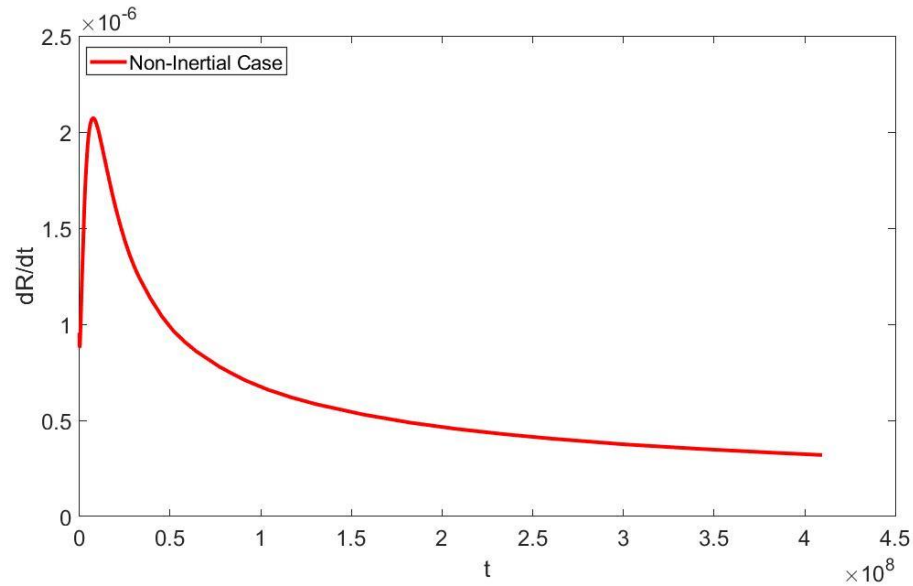**Figure 3-2: Pressure variation inside the bubble**

Figure 3-3: Bubble interface velocity

3.2 Including Inertia in the Bubble Growth Model.

In this section, the effect of liquid inertia from the surroundings on the bubble is explored. Inertia has been neglected in the literature because the effect of it on the bubble growth is negligible compared to concentration gradients (Elshereef et al. (2010)). However, it is interesting to see the effect of inertia together with diffusion on this type of problem (in polymers).

Therefore, one can solve the complete coupled second-order ordinary differential equation (2.55) and (2.57) subjected to the initial conditions (2.59-2.61). The magnitudes of the non-dimensional numbers remain the same as in the non-inertial case i.e. $\text{Re} = 4.5 \times 10^{-6}$, $\text{Ca} = 13.17$, $Z=1.27$, $I = 0.3$, and $\text{Pe} = 3.7 \times 10^{4}$. The comparison between the non-dimensional magnitudes i.e. Reynolds number and Peclet number justifies the reason for neglecting the inertia of the polymer solution where the magnitude of the Reynolds number is no nearer to the Peclet number.

The comparisons of non-dimensional bubble radius, bubble interface velocity, and pressure variation inside the bubble with time are shown in Figure (3-4) to (3-6) respectively. As it was discussed in the above paragraph, these figures show that the effect of inertia is negligible in the case of polymers. This suggests that the bubble growth is rather dominated by the diffusion process rather than inertia.

In Figure (3-5), the initial velocity of the bubble interface for the non-inertial case has nonzero value and on the other side, for inertial growth, the imposed initial value is zero. Yet, the overall trend and the peak magnitudes are the same for both cases. This suggests that the magnitude of the initial velocity of the bubble does not affect the overall bubble growth process.
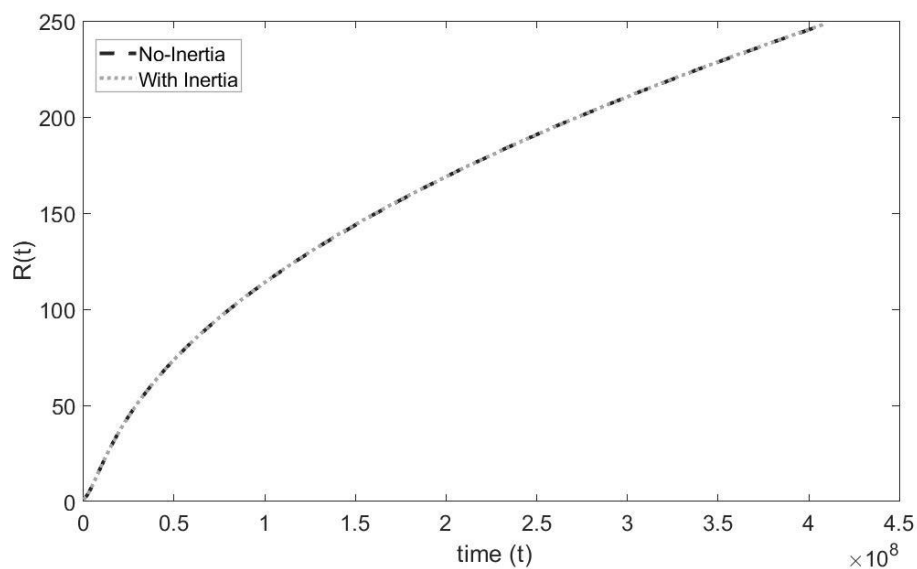
Figure 3-4: Bubble growth comparison for inertial and non-inertial case
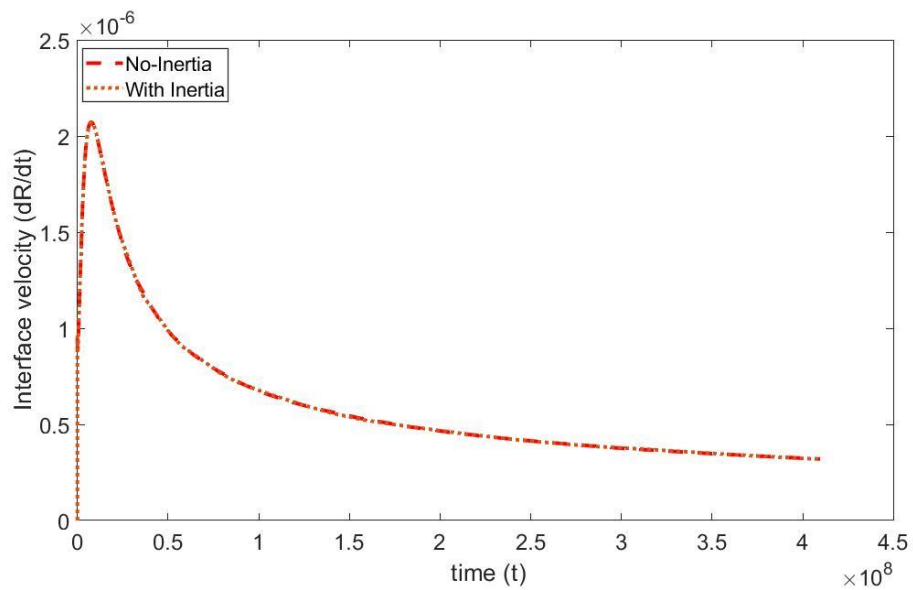
Figure 3-5: Bubble interface velocity comparison with inertial and non-inertial cases
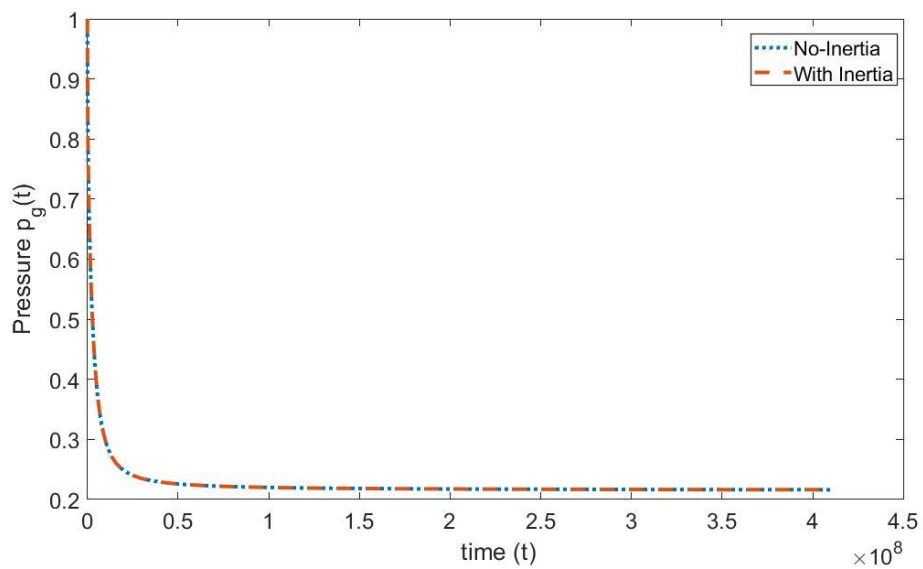
Figure 3-6: Comparison of pressure variation inside the bubble for inertial and non-inertial cases.

3.3 Numerical Solution to the Scalar Advection-Diffusion Equation

This section starts primarily with a grid convergence test to the scalar advection-diffusion equation (2.58). After that, the numerical results from the present model are compared with the Elshereef et al. (2010) bubble growth models. Thereafter, a clear insight into the concentration of gas in the liquid is given and finally, we end this section by comparing the present developed numerical model with the experiment and other bubble growth models.

3.3.1 Grid Independence Test

For the numerical simulations, the infinite spatial domain is assumed to be 10 times the maximum radius of the bubble. And the maximum radius of the bubble is anticipated from Figure (3-1) and dimensionally it is 250 µm. This suggests that the physical infinity of the domain is $250 \times 10 = 2500$ µm and in terms of x_∞ it is 2250 (Note that $x = r - R(t)$).

Grid independence test resolves the potential numerical errors associated with the grid spacing. The idea of this test is to make the numerical solution independent of the grid space. Figure (3-7) shows the grid converges with increasing the number of divisions. It is seen that between the 100 and 1000 divisions there is a larger amount of variation in the magnitude of bubble radius i.e. $\left(\dfrac{R_{1000} - R_{100}}{R_{1000}} \right) > 15\%$, further refinement of the domain from 1000 to 3000 grid cells, the radius of the bubble converged and the margin of error is calculated less than 2%. Therefore, to achieve accurate results in the numerical simulations, the domain is equally discretized with 3000 nodes.
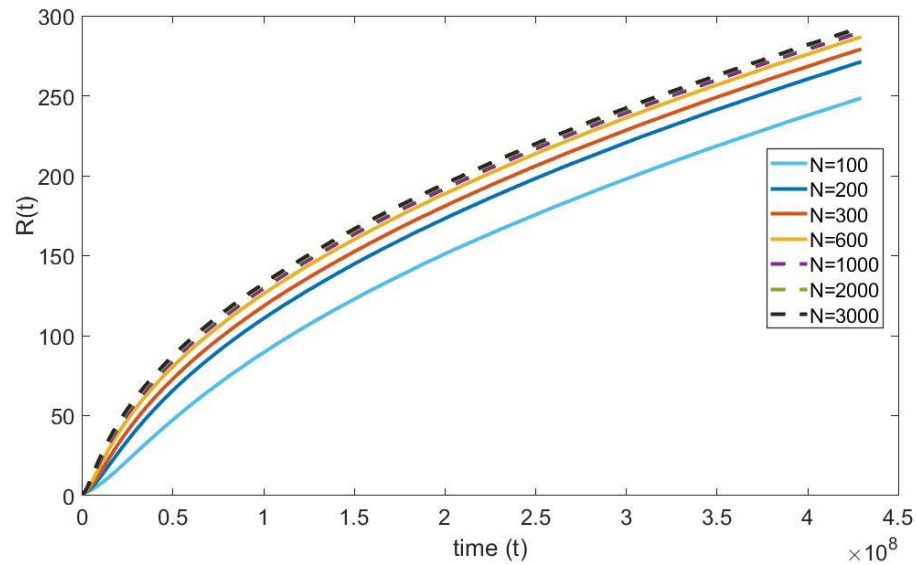
Figure 3-7: Grid Independence Test of the Diffusion equation

3.3.2 Comparison of Present Numerical Model with the Approximate Solution

Until now, the bubble growth dynamics were studied based on the approximate solution to the diffusion equation. In this section, the developed numerical model results (equation 2.55,2.56 and 2.58) are compared with the results of the Elshereef et al. (2010) models which comprise of the equations (2.55) and (2.57).

From Figure (3-8), it is seen that the growth rate of the bubble is predicted higher with the numerical model than the approximated analytical model. The numerical model predicts the bubble radius close to 300 µm. On the other hand, the approximated analytical model predicts the maximum radius of 230 µm. The difference in the growth behavior can be understood from Figure (3-9), where initially the interface velocity of the bubble for the numerical model is comparatively higher than the analytical model. This behavior signals

that at the initial stage's diffusion of gas into the bubble is underestimated by the approximated diffusion solution.
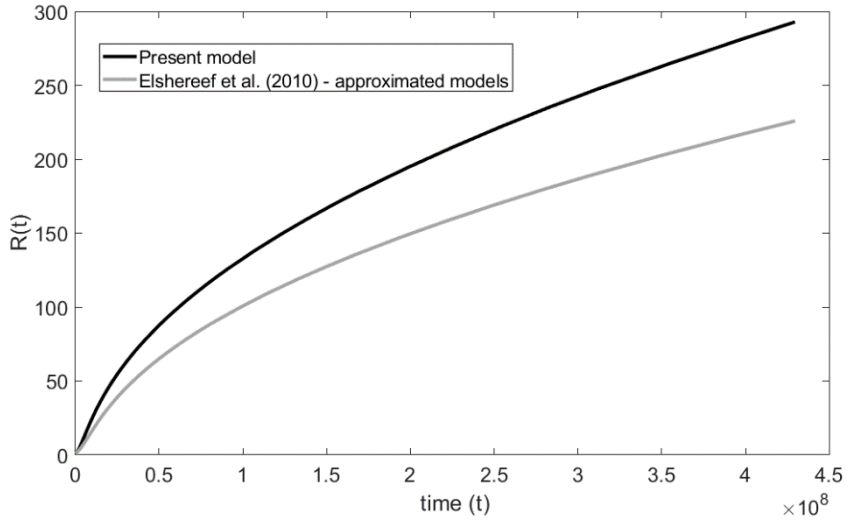

Figure 3-8: Bubble growth comparison between present and approximated model.
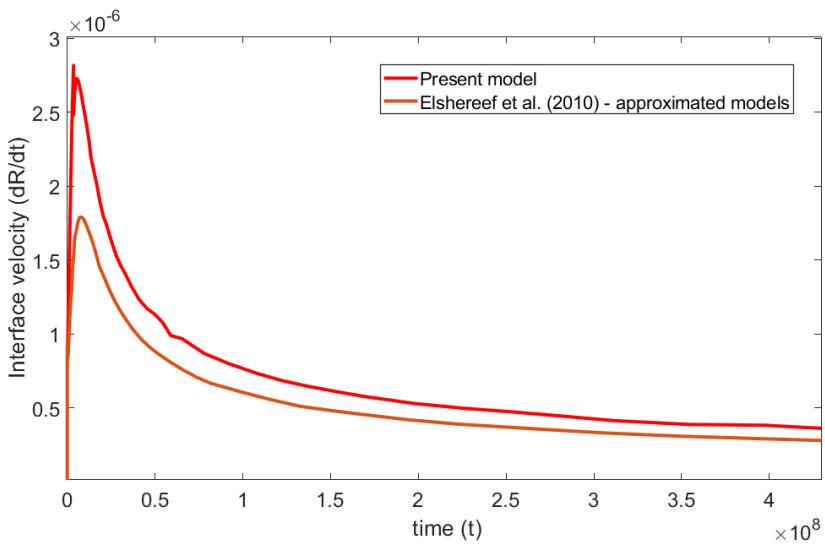

Figure 3-9: Bubble interface velocity comparison between present and approximated models

3.3.3 Concentration in the Liquid

So far in the literature, the variation of concentration of gas in the liquid side has not been reported and investigated properly. For instance, Elshereef et al., (2010) reported that his second comparison model which is developed by Amon and Denson (1984) has solved the advection-diffusion equation using finite difference approximation. However, the concentration profiles in the boundary layer on the liquid side have not been reported. In this section, we present the concentration profile of the gas in the liquid explicitly.

In Figure (3-10), the concentration profiles with time at different locations starting from the interface to a position x=400 are shown. Here x= 400 represents the end of the boundary layer. The boundary layer length is the space between the interface and the position x where the concentration gradients can be observed.

Similarly, in Figure (3-11) the variation of the concentration profile with space at different time steps is shown. From the numerical results, it has been noted that the non-dimensional distance from the interface to the position where the concentration gradient no longer exists is 399.13, which is 3.9913×10^{-4} m in dimensional length.

It is expected that as we move further away from the interface towards infinity, the concentration gradient will be decreasing, and this trend can be observed from Figure (3-10). One can find the cumulative boundary layer length (399.13) from Figure (3-9). To find the instantaneous boundary layer thickness, one has to subtract the bubble radius at that instance from the cumulative boundary layer length.
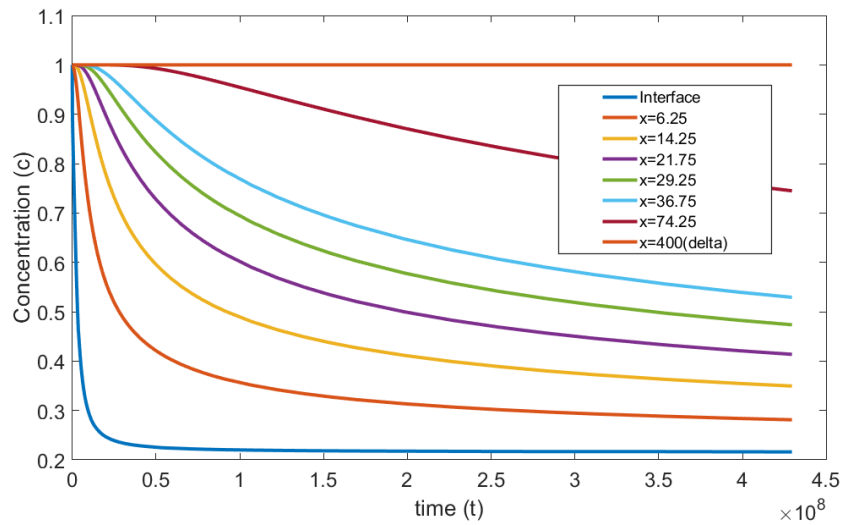
Figure 3-10: concentration profiles reported at different positions with time
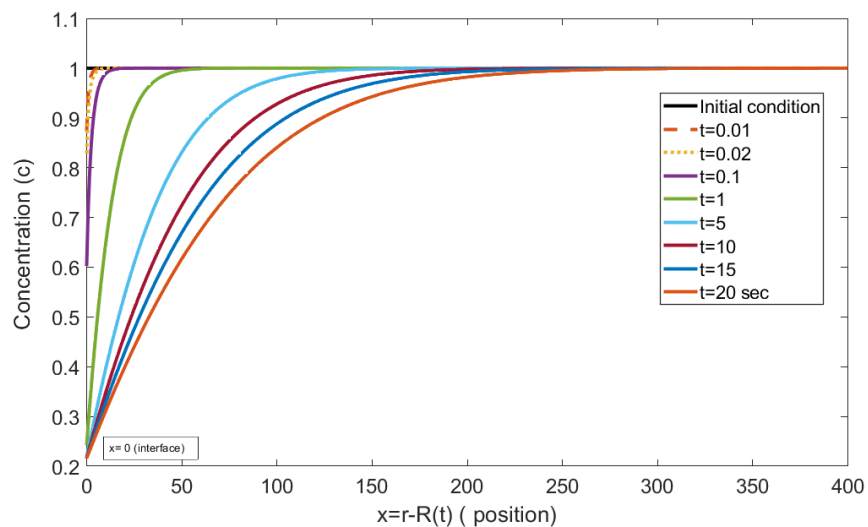

Figure 3-11: Concentration profiles reported in the liquid at different time values

3.3.4 Concentration Profile & Boundary Layer Comparison

As discussed earlier in section 2.5, a parabolic profile in the boundary layer thickness (see equation 2.37) was assumed in the literature to find the approximate solution to the diffusion equation. In this context, a comparison is made between the classical concentration profile that has been reported in the literature and the concentration profile

that has been obtained in the current study. To do so, the concentration profile equation (2.37) in non-dimensional form and in terms of x coordinate takes

$$c(\mathrm{x},t) = c_0 - (c_0 - c_R)\left(1 - \frac{x}{\delta}\right)^2.$$
(3.2)

Figure (3-12) shows the concentration profiles at different times, between the current numerical study (solid lines) and the assumed concentration profile (dashed lines). It is found that the equation (3.2) deviates from its square form when it is compared with the numerical solutions. The numerical profile turned out to be much steeper than the approximated profile, and the numerical data fits with power 5.5 rather than power 2 in the equation (3.2). Therefore, the obtained numerical concentration profile takes the form

$$c(\mathrm{x},t) = c_0 - (c_0 - c_R)\left(1 - \frac{x}{\delta}\right)^{5.5}.$$
(3.3)

In Figure (3-13), a single profile comparison is made at t = 20 sec to emphasize the difference between the equation (3.2) and (3.3). It is noticeably evident that the approximate solution underpredicted the concentration of gas diffusing through the interface into the bubble.

To supplement the above statement, a boundary layer comparison is made between the numerical study and literature. According to Moreno Soto et al., (2019) a diffusive boundary layer is developed around the bubble as it expands and has the value

$$\bar{\delta} = \sqrt{\pi D \bar{t}}.$$
(3.4)

Note that the equation (3.4) does not account for the convection and inertia that caused due to movement of the interface of bubble. Figure (3-14) and Table (3-2) show the dimensional boundary layer plot and values between the current study, equation (2.39), and (3.4) respectively. It has been observed that the numerical simulation (red line) has predicted a larger boundary layer around the bubble than the others. The results seem convincing because in the numerical investigation the full equation is solved whereas in the literature convection part of the diffusion equation is neglected.
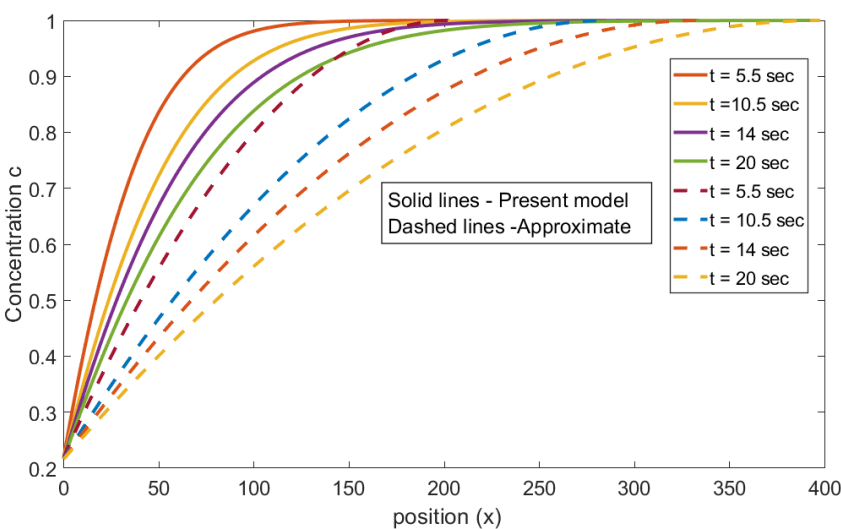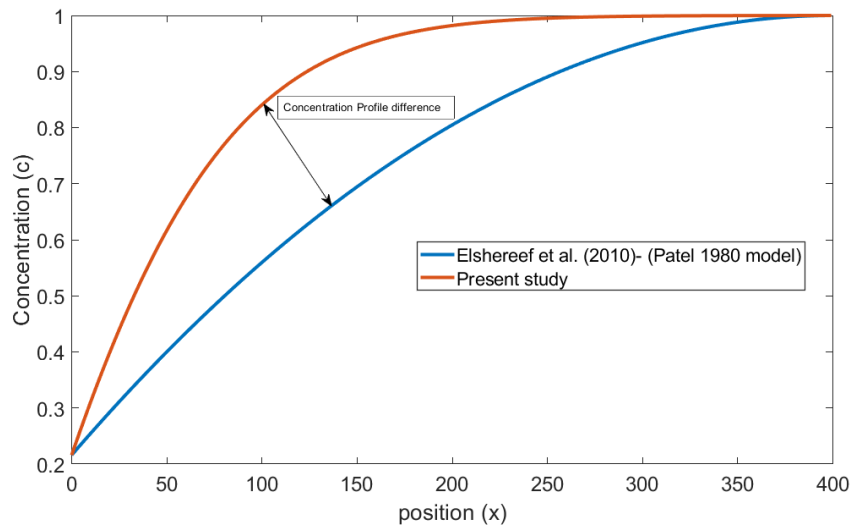

Figure 3-12: Concentration profile comparisons

Figure 3-13: Concentration profile variation with literature assumed profile

Table 3-2: Values of boundary layer thickness comparison

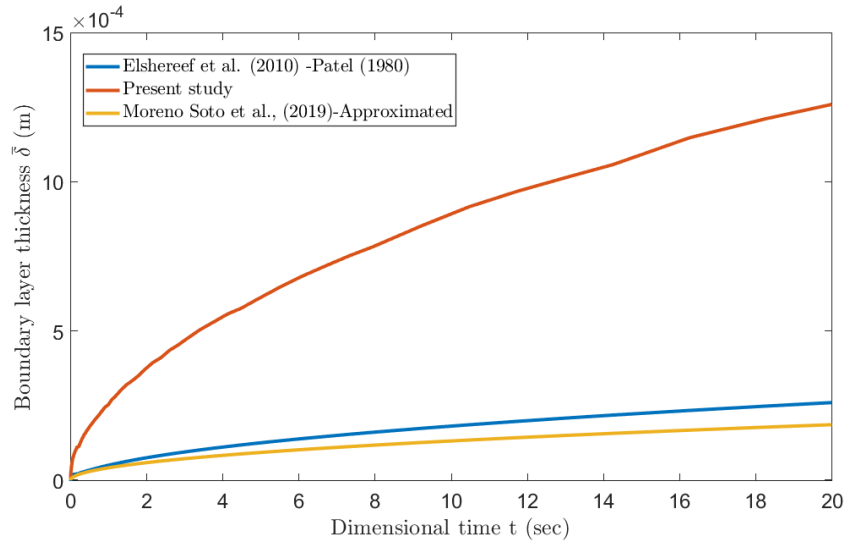| Time $\bar{t}$ sec	Boundary layer thickness Numerical $\bar{\delta}$	Approximated $\bar{\delta}$	Theory $\bar{\delta}$
5sec	5.7e-04	1.35e-04	9.7e-05
10	8.8e-04	1.83e-04	1.34e-05
14 sec	1.0e-03	2.22e-04	1.55e-04
20 sec	1.3e-04	2.6e-04	1.85e-04

Figure 3-14: Boundary layer thickness comparisons

3.3.5 Comparison with Existing Experiments and Theory

A thorough analysis of the bubble hydrodynamics has resulted in producing promising outcomes. The present section focuses on the comparison between the numerical model developed in this work with the available theory and experimental data.

Elshereef et al., (2010) stated that the bubble growth model developed by Patel (1980) and the numerical model developed by Amon and Demson (1986) were not able to justify the experimental data of Han and Yoo (1981). However, his study shows that Amon and Denson's model was able to predict Han and Yoo experiment data much closer than the Patel model.

A comparison was made between the present model and experiment data of Han and Yoo (1981) along with the Patel (1980) and Amon and Denson models in Figure (3-15). It is evident that from the plot the present numerical model was able to capture the experimental

data accurately than the other two models. At the initial stages, it has been observed that there is a discrepancy between the bubble growth models when compared to the experimental data of Han and Yoo (1981). This type of divergence at the initial stage is expected, since the polymer used by Han and Yoo for the experiment exhibits the viscoelastic effect, whereas other numerical models stated in the thesis including the present numerical model and were developed based on pure Newtonian fluid assumptions.

Similarly, in Figure (3-15), the present model and experimental data were compared with Amon and Denson bubble growth model. It has been observed that at initial stages the trend of the model proposed by Patel and Amon and Denson were similar and at later stages, Amon and Denson's model deviates from the Patel model and move towards the present numerical model. Overall, the present model shows more promising and accurate predictions than previous models.
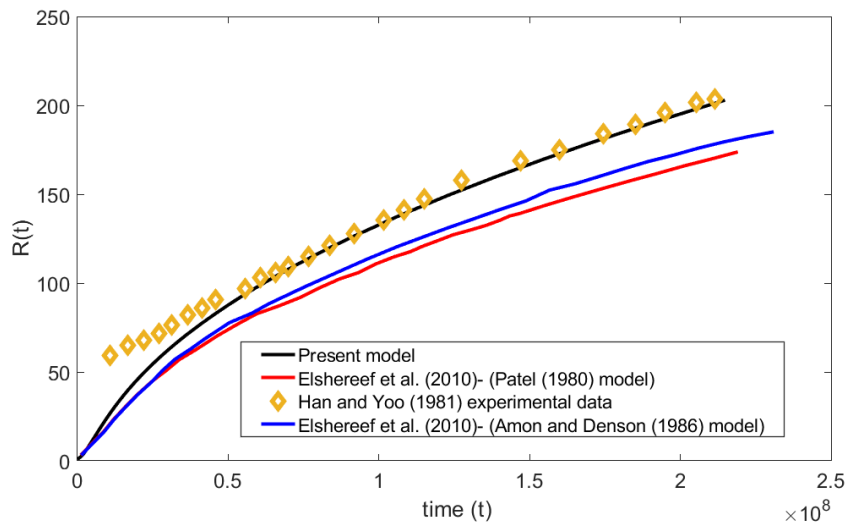

Figure 3-15: Present model comparison with experiment and theory

3.4 Parametric Study of Bubble Growth

Equations (2.55), (2.56), and (2.58) which constitutes the full bubble growth model emphasize that Re, Ca, Pe, Z, and I are the numbers that control the bubble growth. These non-dimensional numbers relate to the physical parameters like an initial bubble size, viscosity of the liquid, surface tension of the liquid, diffusivity of gas and solubility, etc. A small change in these field parameters may affect the bubble growth. In the present section, an extensive study is carried out to see the effect of these parameters on bubble growth.

To do so, we only change a single parameter in non-dimensional numbers which is independent of other non-dimensional numbers. For example, to study the effect of viscosity of the liquid, we only change the μ_L parameter in the Reynolds number equation (2.53a), and to study the effect of surface tension we only change the σ in the Capillary number equation (2.53b) and so on.

To observe the effects of these parameters, we need a primary or base case result to perform a relative comparison. Therefore, we consider the present numerical model results shown in Figure (3-8) as the primary case.

3.4.1 Effect of viscosity on the bubble growth

To see the effect of viscosity, only Reynolds number is varied, keeping other non-dimensional numbers constant as we discussed in the earlier section. By the definition of Reynolds number (see equation (2.53a)), higher the Reynolds numbers lower the viscosity and vice versa. In the base case, the Reynolds number is 4.5×10^{-6}, and this number is varied as low as 4.5×10^{-7} and high as 4.5×10^{-5}.

In Figure (3-16), at higher Reynolds numbers ($\mathbf{Re} = 4.5 \times 10^{-5}$), the bubble growth is higher and at lower Reynolds numbers ($\mathbf{Re} = 4.5 \times 10^{-7}$), the bubble growth is slower. This type of behavior is predicted because, at lower viscosity, the normal stress in the liquid will be lower which results in a faster and higher bubble growth rate. On the other hand, if the viscosity is high, the normal stress will be high which retards the bubble growth. This behavior can be well understood from Figure (3-17), where the initial interface bubble velocity is high at higher Reynolds number, suggesting a rapid bubble growth. And also, at lower Reynolds number, retardation of bubble interface velocity is seen, expressing that the bubble growth rate is slower.

The variation of pressure can be noticed between the high and low Reynolds numbers in Figure (3-18). Lower the Reynolds number lower the reduction of pressure in the bubble which in turn lowers the bubble growth. Consequently, at high Reynolds number, the pressure inside the bubble decreases rapidly suggesting that the bubble is grown very rapidly.
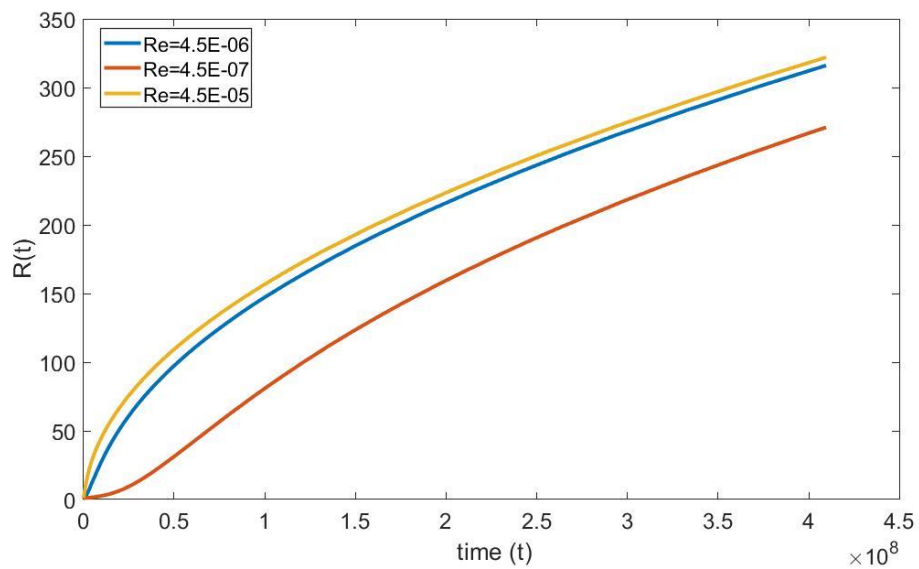
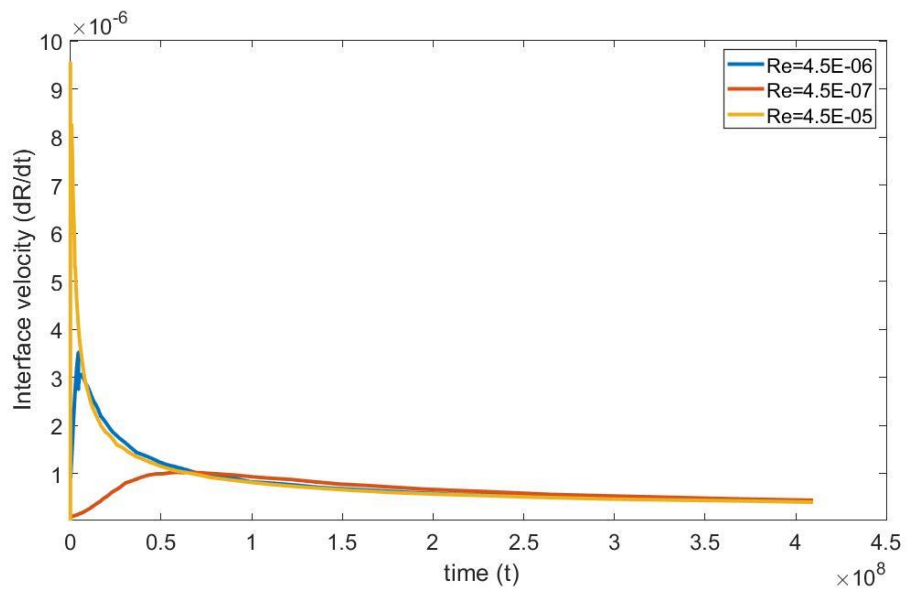**Figure 3-16: Effect of Reynolds number on bubble radius**

Figure 3-17: Effect of Reynolds number on bubble interface velocity
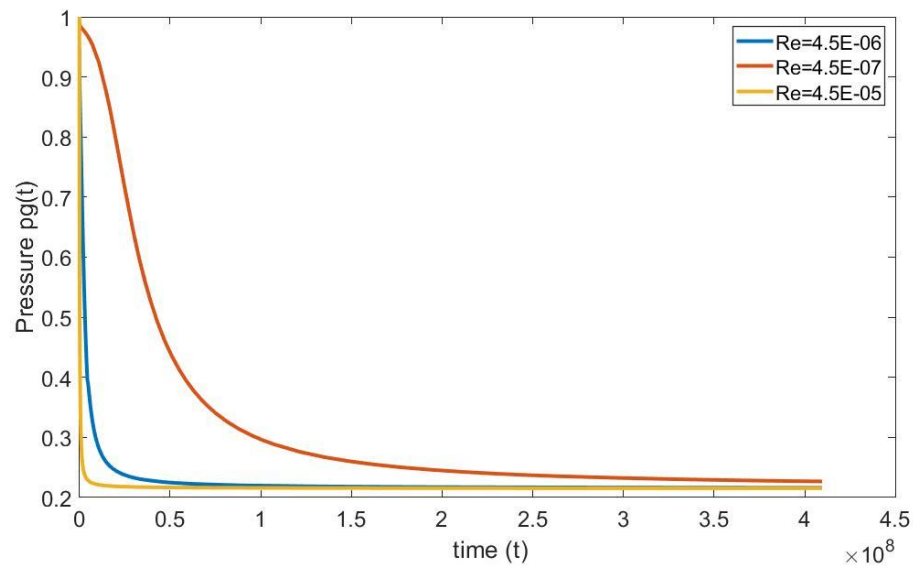
Figure 3-18: Effect of Reynolds number on the pressure inside the gas

3.4.2 Effect of surface tension of the liquid on the bubble growth

The effect of surface tension on the bubble growth is carried out with a similar approach that was demonstrated in the previous section. Capillary number is varied from the reference number keeping other non-dimensional numbers constant. The reference capillary number is 13.17 and is varied in the range of low magnitude (Ca =3) and high magnitude (Ca = 23).

Similar to the varying Re case discussed in the previous section, here, higher the Ca, lower the surface tension, and vice versa. It is expected that the interfacial tension tries to retard the bubble growth by opposing the motion of the bubble boundary and similar behavior is observed from the numerical simulations.

From figures (3-19) -(3-21), at higher Ca, a considerable change in the bubble growth has not been observed. However, there is evidence that at lower Ca, the bubble growth rate is retarded.
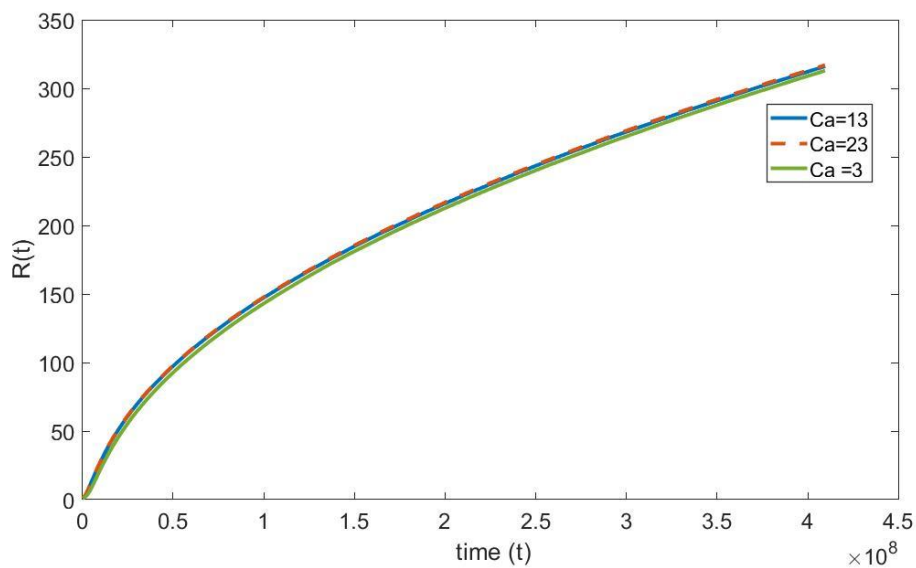

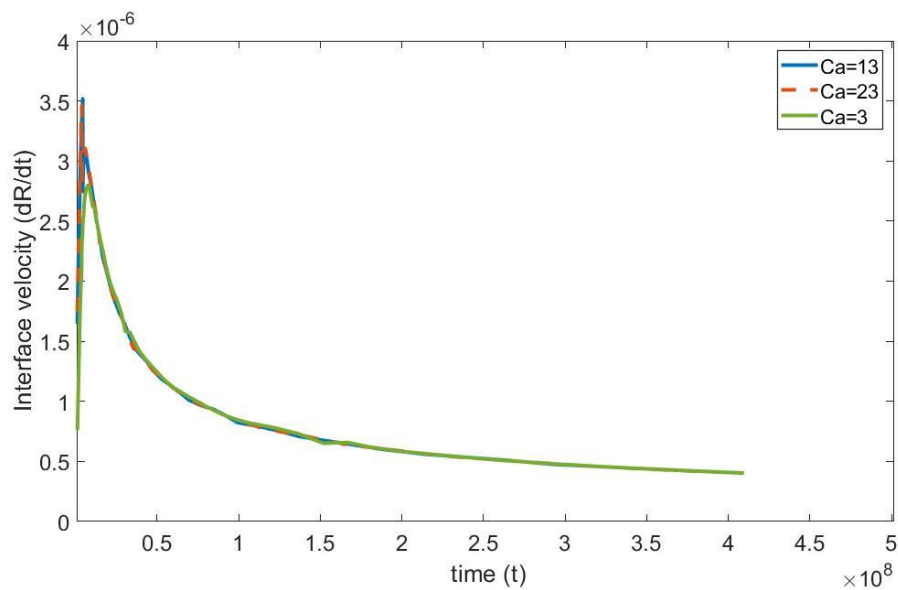**Figure 3-19: Effect of Ca on Bubble growth**

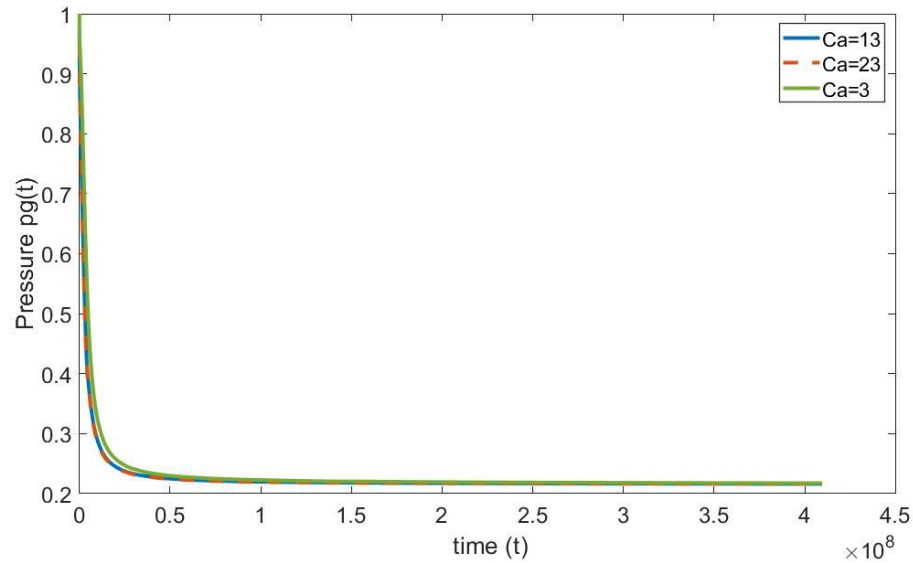**Figure 3-20: Effect of Ca on bubble interface velocity**

Figure 3-21: effect of Ca on Pressure inside the bubble

3.4.3 Effect of system pressure on bubble growth

In this section, the effect of system pressure Pa is studied. The system pressure is the ambient pressure where growth of the bubble takes place. For instance, in the case of foaming, the system pressure is considered as the mold pressure, where bubble growth occurs upon injecting polymer melts in it (Han and Yoo 1981). Similarly, in carbonated beverages, system pressure can be referred to as the ambient pressure.

It is important to see how system pressure affects the overall growth of the bubble. Therefore, three cases were taken, in which one is the reference case P_a=0.21 (polymer mold case), the case of high-pressure P_a =0.31, and the lower pressure case P_a=0.10. Note that the initial gas pressure (p_{g0}) in the bubble is kept constant for all the cases.

One can see from the equation (2.55) the initial magnitude of $\left(p_g - p_a \right)$ defines the rate of

bubble growth. Since the initial pressure $p_g = p_{g0}$ is the same for all the cases, and $p_{g0} >$

p_a, higher the p_a, lower will be the pressure difference and lower will be the bubble

growth.

There is a clear indication from the Figures (3-22) – (3-24), as the system pressure

increases, the bubble growth decreases, and vice versa. On decreasing the system pressure,

it was observed that there was a large deviation between the base case and lower system

pressure case. On the other hand, while increasing the system pressure, it was observed that

there was a comparatively smaller deviation between the base case and lower system
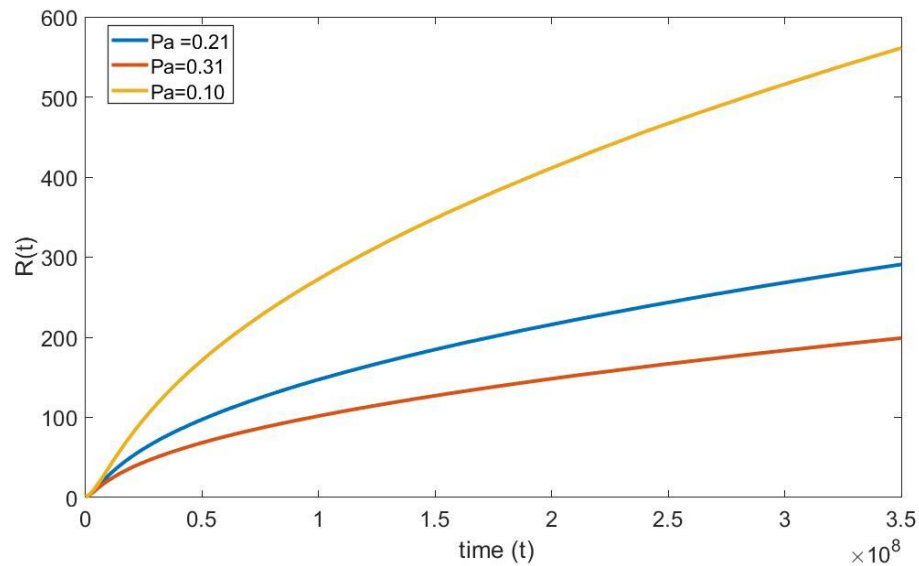
pressure case.

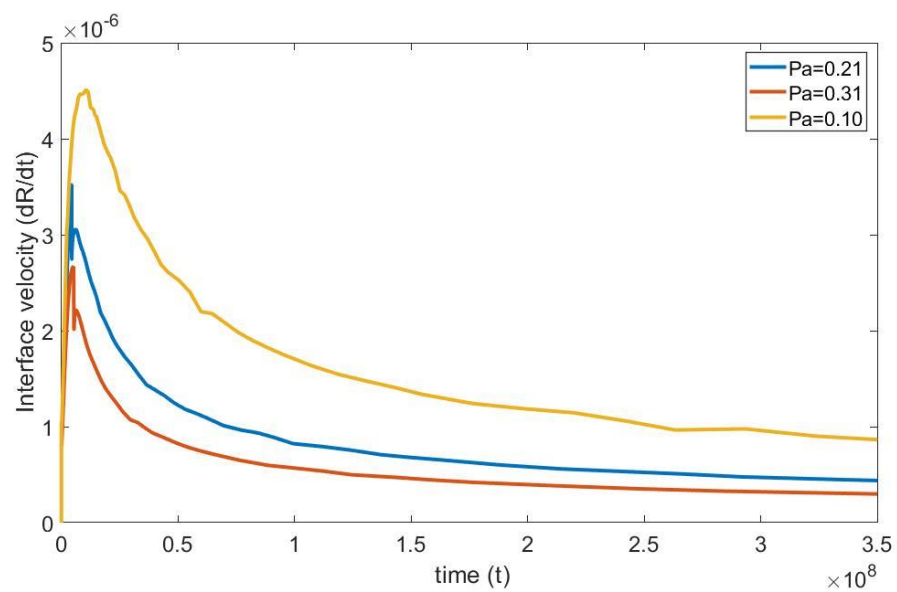
Figure 3-22: Effect of system pressure on bubble growth

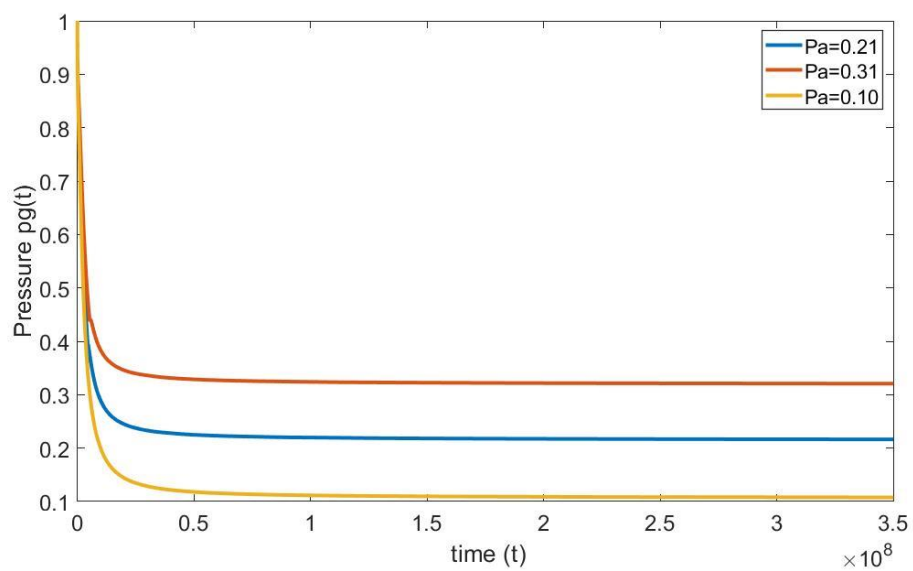**Figure 3-23: Effect of system pressure on bubble interface velocity**

Figure 3-24: Effect of system pressure on the gas pressure inside the bubble

3.4.4 Effect of Solubility and Diffusion Parameters on Bubble Growth

Solubility and diffusivity of the gas in the liquid solution plays a major role in the bubble growth process. The present part focuses on studying the effect of both parameters. From the definition of Peclet number (2.53c), only the diffusion coefficient is varied to maintain the other numbers unchanged.

Therefore, a lower $Pe = 3.7 \times 10^3$ (high diffusion coefficient) and higher Peclet number $Pe = 3.7 \times 10^5$ (low diffusion coefficient) are considered. The magnitudes are compared with the base case, whose Peclet number magnitude is 3.7×10^4. Figure (3.25) shows that at a lower Peclet number, the growth rate of the bubble is higher and at higher Peclet number the growth rate is slower. This type of trend is predicted since at a higher diffusion coefficient, the rate of gas flow through the interface is high and vice versa.

Similarly, to see the effect of solubility on the bubble growth, the non-dimensional number I (see equation (2.54b)) which relates to the Henry's constant k_h is varied. Here, the non-dimensional number I increases on increasing k_h and decreases by decreasing the k_h. The magnitude of the non-dimensional number I for the base case is 0.33 and this is varied between the lower number $I = 0.1$ to a higher number $I = 1$.

Figure (3-26) suggests that, on increasing the solubility of a gas in the liquid, the bubble growth rate is faster and lower the solubility of the gas in the liquid, lower will be the growth rate. This result is close to the physical observations i.e., at higher solubility, the

amount of gas available in the liquid will be high, due to which the mass transfer from the liquid side to the bubble will be high resulting in a higher bubble growth rate.

From the results, an interesting phenomenon has been observed i.e. the effect of diffusion and solubility are closely related. From Figure (3-27), both the cases of diffusion and solubility effects on the bubble growth are shown. It indicates that the effect of these parameters is almost similar to overall bubble growth.
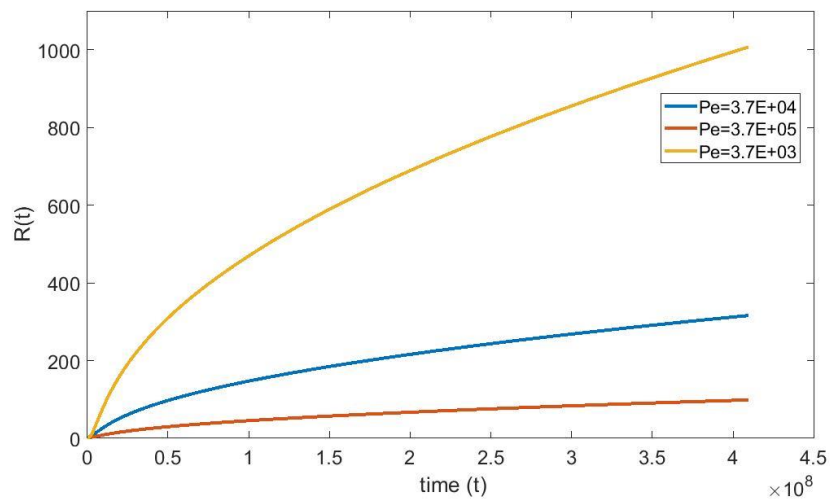

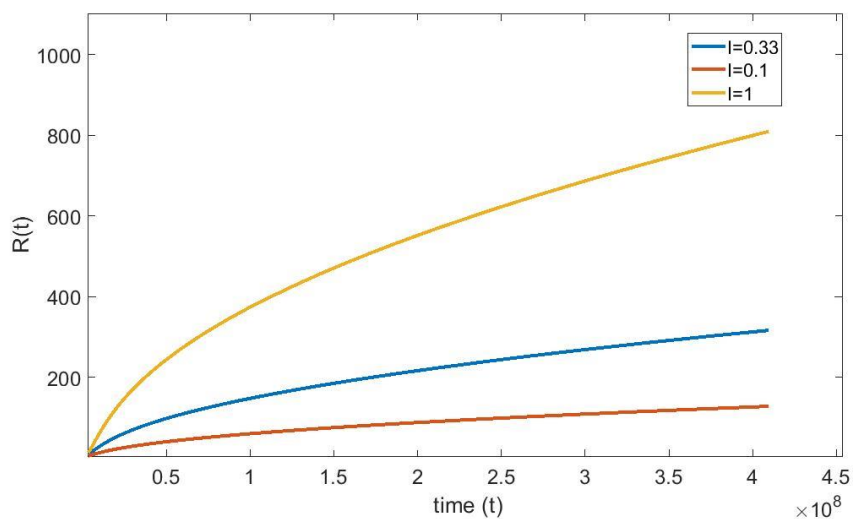**Figure 3-25: Effect of diffusion coefficient on bubble growth**

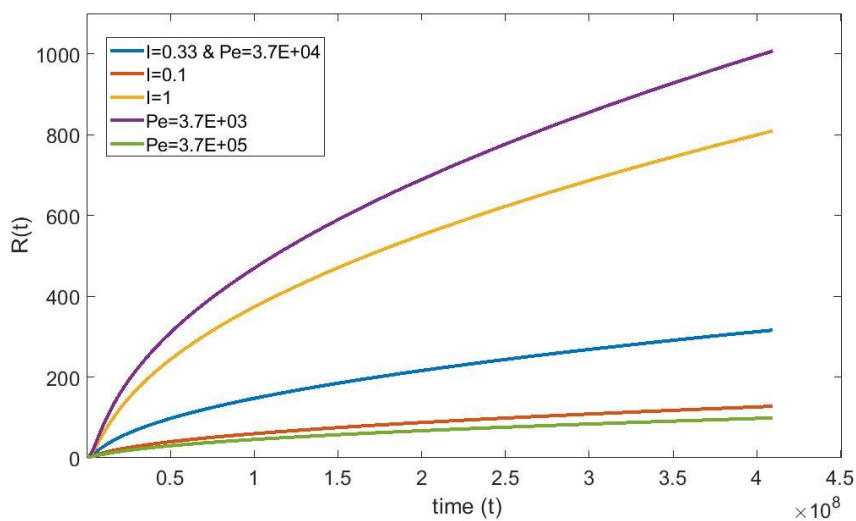**Figure 3-26: Effect of Henry's constant on bubble growth**

Figure 3-27: Relation between diffusion and solubility of a gas in the liquid

3.5 Summary

To summarize, the numerical approach adopted to solve the system of non-linear coupled equations were validated qualitatively and quantitatively by reproducing the results of non-inertial bubble growth from Elshereef et al. (2010). The numerical solution was carried out to the complete scalar advection-diffusion equation and compared with the classical approximated solution. It has been observed that the numerical solution predicted higher bubble growth. The comparison of present results with the experimental data of Han and Yoo (1981) suggested that the present results accurately predicated growth in comparison to the available theory.

 The effect of viscosity, surface tension, system pressure, diffusion, and solubility of the gas on the bubble growth was studied. It was observed that surface tension played a minimal role in the bubble growth, whereas viscosity and system pressure had a significant

effect. The numerical results suggested that the effect of diffusion and solubility contributes equally to the bubble growth effect.

Chapter 4

4 Concluding Remarks

The hydrodynamics of a single bubble in the pool of Newtonian liquid that expands due to mass transfer is investigated in the current thesis. This study directly relates to the foaming process, carbonated beverages, and any other problem in which the bubble grows due to mass transfer.

Rigorous non-dimensional formulations were derived to incorporate interfacial, viscosity, diffusivity and solubility effect on bubble growth. Especially the inertia of the liquid is included in the formulation along with the full scalar advection-diffusion. A strong numerical approach to the highly non-linear stiff coupled equations was discussed. The moving interface of the bubble is tackled by mapping the domain to the new coordinate (x).

The non-inertial hydrodynamic formulation from literature is rederived and the results were reproduced to validate the numerical methodology that is adopted for this thesis. Thereafter, inertia is added to the literature formulation, in which an approximate solution is used for the advection-diffusion equation. An attempt is made to study why inertia does not affect bubble growth in highly viscous liquids like polymer melts.

The results obtained with the present formulation and numerical solution to the advection-diffusion equation were compared with the Elshereef et al. (2010) models. The present numerical model predicts accurate bubble growth in comparison to Elshereef et al. (2010) models. These results were validated by comparing with the Han and Yoo (1981) experimental data set.

It has been never reported in the literature about the behavior of the concentration of gas in the liquid. In this thesis, a clear insight is provided on the concentration profiles of gas in the liquid and a boundary layer variation around the bubble. A simple numerical investigation was conducted to show the variation of the approximated diffusion equation results with the present numerical results. It has been shown that the concentration of the gas profile in the liquid deviates from equation (3.2).

With the validated numerical model, an intensive parametric study was carried on the bubble growth. The results show that the rate of bubble growth primarily depends on the viscosity of the liquid, initial pressure difference, diffusion, and solubility. The effect of surface tension has a limited effect on the overall bubble growth process.

It has been concluded that the higher viscosity of the liquid will lower the bubble growth rate and vice versa. The initial pressure difference between the bubble and the system has a huge impact on the overall bubble growth process. Higher the initial pressure difference, greater is the bubble growth, and with lower initial pressure difference the bubble growth is limited.

The investigation shows that the effect of diffusion and solubility of the gas in the liquid plays an important role in the overall bubble growth process. Higher the magnitude of these parameters, the higher will be the bubble growth rate, and vice versa. It is concluded that these parameters have a similar effect on bubble growth.

4.1 Future work

The present thesis can be extended to the process where the bubble expands due to mass and heat transfer processes. A similar numerical approach that has been carried out to the

advection-diffusion equation can be applied to the energy equation. More accurate discretization methods like finite element method, finite volume method, and spectral analysis can be adopted to solve the scalar diffusion equation and the one-dimensional problem can be expanded to two-dimensional axisymmetric.

In the present thesis, the effect of the viscoelasticity of the fluid (polymers) is not included in the hydrodynamic equation, which can be incorporated in future work.

References

Allen, J. S. and Roy, R. A. (2000) 'Dynamics of gas bubbles in viscoelastic fluids. II. Nonlinear viscoelasticity', *The Journal of the Acoustical Society of America*, 108(4), pp. 1640–1650.

Amon, M. and Denson, C. D. (1984) 'A study of the dynamics of foam growth: Analysis of the growth of closely spaced spherical bubbles', *Polymer Engineering & Science*, 24(13), pp. 1026–1034.

Arefmanesh, A. and Advani, S. G. (1991) 'Diffusion-induced growth of a gas bubble in a viscoelastic fluid', *Rheologica Acta*. Springer, 30(3), pp. 274–283.

Arefmanesh, A., Advani, S. G. and Michaelides, E. E. (1992) 'An accurate numerical solution for mass diffusion-induced bubble growth in viscous liquids containing limited dissolved gas', *International Journal of Heat and Mass Transfer*, 35(7), pp. 1711–1722.

Barker, G. S., Jefferson, B. and Judd, S. J. (2002) 'The control of bubble size in carbonated beverages', *Chemical Engineering Science*, 57(4), pp. 565–573.

Barlow, E. J. and Langlois, W. E. (1962) 'Diffusion of Gas from a Liquid into an Expanding Bubble', *IBM Journal of Research and Development*, 6(3), pp. 329–337.

Birkhoff, G., Margulies, R. S. and Horning, W. A. (1958) 'Spherical bubble growth', *Physics of Fluids*, 1(3), pp. 201–204.

Bisperink, C. G. J. and Prins, A. (1994) 'Bubble growth in carbonated liquids', *Colloids and Surfaces A: Physicochemical and Engineering Aspects*, 85(2–3), pp. 237–253.

Brujan, E. and Williams, P. R. (2005) 'Bubble dynamics and cavitation in non-Newtonian

liquids', *Rheology Reviews*, 2005(April 2005), pp. 147–172.

Carslaw, H. S. (1945) *Introduction to the Mathematical Theory of the Conduction of Heat in Solids*. New York: Dover.

Chappell, M. A. and Payne, S. J. (2006) 'A physiological model of the release of gas bubbles from crevices under decompression', *Respiratory Physiology and Neurobiology*, 153(2), pp. 166–180.

Divinis, N. *et al.* (2004) 'Bubbles growing in supersaturated solutions at reduced gravity', *AIChE Journal*, 50(10), pp. 2369–2382.

Elshereef, R., Vlachopoulos, J. and Elkamel, A. (2010) 'Comparison and analysis of bubble growth and foam formation models', *Engineering Computations (Swansea, Wales)*, 27(3), pp. 387–408.

Enríquez, O. R. *et al.* (2013) 'Growing bubbles in a slightly supersaturated liquid solution', *Review of Scientific Instruments*, 84(6).

Enríquez, O. R. *et al.* (2014) 'The quasi-static growth of CO2 bubbles', *Journal of Fluid Mechanics*, 741, pp. 1–9.

Epstein, P. S. and Plesset, M. S. (1950) 'On the stability of gas bubbles in liquid-gas solutions', *The Journal of Chemical Physics*, 18(11), pp. 1505–1509.

Feng, J. J. and Bertelo, C. A. (2004) 'Prediction of bubble growth and size distribution in polymer foaming based on a new heterogeneous nucleation model', *Journal of Rheology*, 48(2), pp. 439–462.

Fogler, H. S. and Goddard, J. D. (1970) 'Collapse of spherical cavities in viscoelastic

fluids', *Physics of Fluids*, 13(5), pp. 1135–1141.

Han, C. D. and Yoo, H. J. (1981) 'Studies on structural foam processing. IV. Bubble growth during mold filling', *Polymer Engineering & Science*, 21(9), pp. 518–533.

Harris, W. D. (1976) 'F', *Plastics eng*, 39(4).

Hernandez-Alvarado, F. *et al.* (2017) 'Void fraction, bubble size and interfacial area measurements in co-current downflow bubble column reactor with microbubble dispersion', *Chemical Engineering Science*. Elsevier Ltd, 168, pp. 403–413.

Hey, M. J., Hilton, A. M. and Bee, R. D. (1994) 'The formation and growth of carbon dioxide gas bubbles from supersaturated aqueous solutions', *Food Chemistry*, 51(4), pp. 349–357.

Jiménez-Fernández, J. and Crespo, A. (2005) 'Bubble oscillation and inertial cavitation in viscoelastic fluids', *Ultrasonics*, 43(8), pp. 643–651.

Jones, S. F., Evans, G. M. and Galvin, K. P. (1999) 'The cycle of bubble production from a gas cavity in a supersaturated solution', *Advances in Colloid and Interface Science*, 80(1), pp. 51–84.

Khayat, R. E. and Garcia-Rejon, A. (1992) 'Uniaxial and biaxial unsteady inflations of a viscoelastic material', *Journal of Non-Newtonian Fluid Mechanics*, 43(1), pp. 31–59.

Kuni, F. M. and Zhuvikina, I. A. (2002) 'A theory of homogeneous boiling-up of liquid solutions: 1. Kinetic equation of boiling-up', *Colloid Journal*, 64(2), pp. 166–171.

Kuni, F. M., Zhuvikina, I. A. and Grinin, A. P. (2003) 'A theory of homogeneous boiling-up of liquid solutions: 3. Growth of supercritical bubbles with allowance for solvent

fugacity', *Colloid Journal of the Russian Academy of Sciences: Kolloidnyi Zhurnal*, 65(2), pp. 201–205.

Lee, S. T., Ramesh, N. S. and Campbell, G. A. (1996) 'Study of thermoplastic foam sheet formation', *Polymer Engineering and Science*, 36(19), pp. 2477–2482.

Lee, W. T., McKechnie, J. S. and Devereux, M. G. (2011) 'Bubble nucleation in stout beers', *Physical Review E - Statistical, Nonlinear, and Soft Matter Physics*, 83(5), pp. 1–5.

Liger-Belair, G. (2005) 'The physics and chemistry behind the bubbling properties of champagne and sparkling wines: A state-of-the-art review', *Journal of Agricultural and Food Chemistry*, 53(8), pp. 2788–2802.

Lin, H., Storey, B. D. and Szeri, A. J. (2002) 'Inertially driven inhomogeneities in violently collapsing bubbles: The validity of the Rayleigh-Plesset equation', *Journal of Fluid Mechanics*, 452, pp. 145–162.

Moreno Soto, Á. *et al.* (2019) 'Transition to convection in single bubble diffusive growth', *Journal of Fluid Mechanics*, 871, pp. 332–349.

Patel, R. D. (1980) 'Bubble growth in a viscous Newtonian liquid', *Chemical Engineering Science*, 35(11), pp. 2352–2356.

Payvar, P. (1987) 'Mass transfer-controlled bubble growth during rapid decompression of a liquid', *International Journal of Heat and Mass Transfer*, 30(4), pp. 699–706.

PES Solutions (no date) *PES-201: Boat Propeller Cavitation And Repair - Plant, Equipment, & Services BlogPlant, Equipment, & Services Blog*, *2014*. (Accessed: 15 July 2020).

Plesset, M. S. and Zwick, S. A. (1954) 'The growth of vapor bubbles in superheated liquids', *Journal of Applied Physics*, 25(4), pp. 493–500.

Pooladi-Darvish, M. and Firoozabadi, A. (1999) 'Solution-gas drive in heavy oil reservoirs', *Journal of Canadian Petroleum Technology*, 38(4), pp. 54–60.

Prosperetti, A. and Plesset, M. S. (1978) 'Vapour-bubble growth in a superheated liquid', *Journal of Fluid Mechanics*, 85(2), pp. 349–368.

Ramesh, N. S., Rasmussen, D. H. and Campbell, G. A. (1991) 'Numerical and experimental studies of bubble growth during the microcellular foaming process', *Polymer Engineering & Science*, 31(23), pp. 1657–1664.

Rosner, D. E. and Epstein, M. (1972) 'Effects of interface kinetics, capillarity and solute diffusion on bubble growth rates in highly supersaturated liquids', *Chemical Engineering Science*, 27(1), pp. 69–88.

Scriven, L. E. (1959) 'on the dynamics of phase growth', *Chemical Engineering Science*, 10.

Sparks, R. S. J. (1978) 'The dynamics of bubble formation and growth in magmas: A review and analysis', *Journal of Volcanology and Geothermal Research*, 3(1–2), pp. 1–37.

Venerus, D. C. and Yala, N. (1997) 'Transport Analysis of Diffusion-Induced Bubble Growth and Collapse in Viscous Liquids', *AIChE Journal*, 43(11), pp. 2948–2959.

Venerus, D. C., Yala, N. and Bernstein, B. (1998) 'Analysis of diffusion-induced bubble growth in viscoelastic liquids', *Journal of Non-Newtonian Fluid Mechanics*, 75(1), pp. 55–75.

Verhaart, H. F. A., de Jonge, R. M. and van Stralen, S. J. D. (1980) 'Growth rate of a gas bubble during electrolysis in supersaturated liquid', *International Journal of Heat and Mass Transfer*, 23(3), pp. 293–299.

W.Zijl, D.Moalem, S. J. D. van S. (1977) 'Inertial and Diffusion Controlled Bubble Growth and Implosion in Initially Uniform Pure and Binary Systems', *Letters in Heat and Mass transfer*, 4(9), pp. 331–339.

Wang, Z. and Bankoff, S. G. (1991) 'Bubble growth on a solid wall in a rapidly-depressurizing liquid pool', *International Journal of Multiphase Flow*, 17(4), pp. 425–437.

Wild, G. (2003) 'Some Aspects of the Hydrodynamics of Bubble Colmuns', *International Journal of Chemical Reactor Engineering*, 1.

Xu, D. *et al.* (2005) 'Fundamental study of CBA-blown bubble growth and collapse under atmospheric pressure', *Journal of Cellular Plastics*, 41(6), pp. 519–538.

Zhuvikina, I. A. and Kuni, F. M. (2002) 'A theory of the homogeneous boiling-up of liquid solutions. 2. The steady-state rate of boiling-up', *Colloid Journal*, 64(5), pp. 556–561.

Curriculum Vitae

Name:	Raj Kumar Nayak Maloth
Post-Secondary Education and Degrees:	CMR College of Engineering and Technology, Telangana, India (2013-2017)
Honours and Awards:	Western Engineering Scholarship 2018-2020
	Undergraduate Engineering Scholarship 2013-2017
Related Work Experience:	Research and Teaching Assistant
	Western University, London, Ontario, Canada (2018-2020)
	Process Executive
	Spectrum Consultants India Pvt Ltd (2017-2018), Telangana, India